INTERNATIONAL ATOMIC ENERGY AGENCY
UNITED NATIONS EDUCATIONAL, SCIENTIFIC AND CULTURAL ORGANIZATION

INTERNATIONAL CENTRE FOR THEORETICAL PHYSICS
34100 TRIESTE (ITALY) - P.O.B. 586 - MIRAMARE - STRADA COSTIERA 11 - TELEPHONE: 2240-1
CABLE: CENTRATOM - TELEX 460392-1

H4.SMR.203 - 12

" SPRING COLLEGE ON GEOMAGNETISM AND AERONOMY "

(2 - 27 March 1987)

" The MST radar technique: potential for middle atmospheric studies "

presented by :

R.F. WOODMAN
Instituto Geophysico del Peru
Apartado 3747
Lima 100
Peru

Verlag, Basel

The MST Radar Technique: Potential for Middle Atmospheric Studies

By B. B. BALSLEY[1]) and K. S. GAGE[1])

Abstract – We examine the potential of the MST (mesosphere-stratosphere-troposphere) dar technique for obtaining detailed information on the middle atmosphere. This technique – ıich uses very sensitive coherent VHF and UHF radars – is capable of detecting signal returns ising from weak fluctuations in the atmospheric refractive index. With certain limitations the ST technique is capable of continually observing winds, waves, turbulence and atmospheric ıbility over the height range 1–100 km with good-to-excellent time and space resolution. We amine the relatively large body of literature that has been written over the past few years and tline some aspects of a promising future.

Key words: MST radar; Wind observation; Wave observation.

1. Introduction

It has become apparent in the last few years that a complete understanding of ıg-term climatic changes, including possible Sun–weather effects and the effects anthropogenic contamination, requires an understanding of the dynamic processes curring in the region between the tropopause and 100 km – i.e., the middle atmo- here. A coordinated study of this region using a variety of experimental techniques ll take place during the next few years under the auspices of the Middle Atmosphere ogram (MAP). The MST (mesosphere–stratosphere–troposphere) radar technique a recent development that offers a great deal of promise in advancing our under- nding of the middle atmosphere. This technique uses ultrasensitive VHF (30–) MHz) and UHF (300–3000 MHz) radars to study the weak backscattering arising m refractive index fluctuations in the neutral atmosphere and lower ionosphere. alysis of these scattered signals enables measurement of the dynamic properties the atmosphere – winds, waves, turbulence and atmospheric stability – throughout middle atmosphere. While we will refer to the MST radar *technique* in subsequent tions, specific *systems* have been subdivided into either MST or ST (stratosphere– posphere) systems by their operating frequency and/or average power-aperture ducts.

[1]) Aeronomy Laboratory, National Oceanic and Atmospheric Administration, Boulder, orado 80303, USA.

The MST technique is capable of obtaining useful returns over the height range 1–100 km. Echoes coming from heights below approximately the stratopause (≃ 50 km) arise primarily from refractive index fluctuations due to small-scale (one-half the transmitted wavelength) inertial range turbulence. Echoes returned from above the stratopause, which are normally observed only during daylight hours, arise primarily from free electrons that enhance the scattering cross-section of the neutral turbulence fluctuations at these heights. The most difficult region to observe by the MST technique is the region near the stratopause because of the combined effect of the exponentially decreasing atmospheric density and the lack of sufficient free electrons.

The temporal and spatial resolution provided by the MST technique varies with radar sensitivity and with height. A resolution of a few tens of meters and a few seconds is possible when the effective signal-to-noise ratio of the scattered signal is well above unity. Resolution degrades to a few km and tens of minutes when the signal is weakest, for example, near the stratopause.

The advantage of the MST technique over other techniques lies in the continuity of the data in both time and height. The time resolution is orders of magnitude better than rocket or balloon data. Other ground-based techniques (meteor winds, airglow, laser radar, etc.) have poorer time continuity or are sensitive only to specific heights. Thus the advent of the MST technique offers an unparalleled opportunity to study not only gross features of the total wind field, but also small-scale, time-varying structures such as gravity waves and turbulence throughout the middle atmosphere.

Development of the MST technique has its historical roots in decades of radio propagation experiments, radar probing of the optically clear neutral atmosphere and radar investigations of the ionosphere by the thermal (also known as incoherent or Thomson) scatter technique. As far as the authors can determine, the first observations of true atmospheric echoes were reported by COLWELL and FRIEND (1936) and WATSON-WATT *et al.* (1937), who used a pulsed HF system to observe a series of scattering layers ranging between 2–60 km. A review of the history of radar probing of the clear atmosphere appears in GAGE and BALSLEY (1978), and a review of the history of thermal (incoherent) scatter has been given by EVANS (1969). Specific references are given in the following sections when appropriate.

2. General considerations of the MST radar technique

a. MST/ST systems defined

Conceptually, the MST technique involves radar backscattering from non-thermal fluctuations in the atmospheric refractive index (for additional discussions of MST/ST concepts, see GORDON, 1978). The pertinent scale size for backscattering is one-half the transmitted wavelength. The non-thermal fluctuations considered here arise primarily from turbulence, although a number of additional processes contribute to the scattering under special conditions. Among these are the stratification of the stable atmosphere into thin layers and the generation of ionized trails by incoming

meteor particles. The first is discussed below in terms of a Fresnel or partial reflection process; the second, which can also be considered in terms of Fresnel reflection, holds the promise of extending MST studies to the nighttime upper mesosphere.

Many of the radars involved in MST studies are also capable of obtaining echoes from thermal fluctuations (i.e., the statistical fluctuations of a medium in thermodynamic equilibrium), provided that the radar is sufficiently sensitive and that the medium contains a sufficient number of free electrons. Scattering from thermal fluctuations in an ionized medium has been variously termed thermal, incoherent, or Thomson scattering (see WOODMAN and GUILLÉN (1974) and RASTOGI and BOWHILL (1976a) for a discussion of thermal versus non-thermal scattering). In this paper, we will adopt the term thermal scattering for incoherent or Thomson scattering while recognizing that the other terms are at least as commonly used in the current literature. The various types of non-thermal scattering will be discussed in terms of their specific mechanisms.

Determination of atmospheric motions by the MST radar technique requires that the radar system be frequency coherent – i.e., that the received signal is mixed with the transmitted frequency to retain both the amplitude and phase of the returned signals. Typical analysis procedures entail obtaining the echo power spectrum of the coherently demodulated returns. Moments of the resulting spectrum yield the echo power, mean Doppler shift, and spectral width. These parameters, in turn, describe respectively the fluctuation intensity, the radial velocity of the scattering medium, and the distribution of random velocities within the scattering volume (WOODMAN and GUILLÉN, 1974).

Radar systems capable of observing non-thermal scattering throughout the entire atmospheric system must be exceedingly sensitive. The rapid decrease of received power with height from the lowest heights to about the stratopause as shown in Fig. 1 (BALSLEY, 1978) is in excess of ten orders of magnitude. The requisite average power-aperture product (average transmitter power capability multiplied by the effective antenna area), which is useful in determining the ultimate sensitivity of an MST system, must be at least 10^9 W m^2. (GORDON (1978) suggests a roughly equivalent value for *peak* power aperture product of 10^{11} W m^2.) An equally important requirement is that the transmitted frequency be sufficiently low so that the scattering scale size normally lies within the inertial subrange of turbulence at all heights (cf. Section 3c), since turbulence on scales smaller than this will be strongly damped by viscous dissipation. This limits the operating frequency of an MST radar to values below at least 100 MHz and preferably below 50 MHz (GORDON, 1978).[2]) Radars operating at higher frequencies or having smaller average power-aperture products that are

[2]) A 30 MHz lower limit for MST radars has been suggested (GORDON, 1978) to preclude the undesirable effects of ionospheric reflection, round-the-world echoes, and HF spectrum pollution. However, the possibility of sounding the middle atmosphere at lower frequencies has been anticipated by WATSON-WATT *et al.* (1937) and may provide a fruitful field for further investigation.

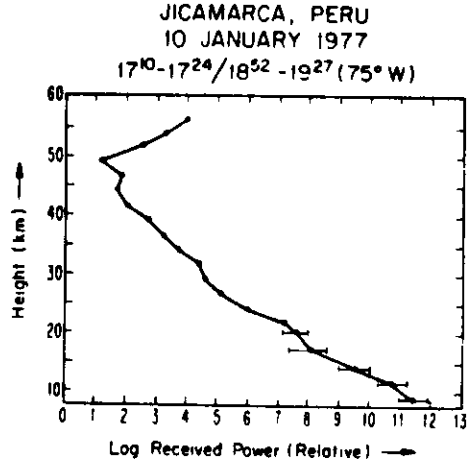

Figure 1
A 49 m nute average of received power vs. height obtained from the Jicamarca Radar Observatory in Peru with the antenna directed $\simeq 1.5°$ south of vertical (on-axis position). Error bars below 20 km arise from matching different profiles. Data points between about 42 km and 52 km are approximate and indicate the maximum possible echo power. The increased echo power above 50 km is due to the presence of free electrons. (After BALSLEY, 1978.)

capable of observing non-thermal scattering at some, but not all, heights have been termed ST (stratosphere–troposphere) radars.

It should be emphasized that the practical delineation between MST and ST radars is not precise. The 10^9 W m^2 average power-aperture product suggested by GORDON (1978) as a minimum value for an MST system enables a radar operating at about 50 MHz to obtain useful data over the complete height range, particularly in the region 45 km ± 15 km where the signal returns are weakest. Systems with smaller power-aperture products are clearly capable of obtaining high-quality mesospheric data above about 60 km, as we will discuss in Section 5. It is only the region near the stratospause that is typically inaccessible to an ST radar operating in the lower VHF.

b. MST/ST facilities

A list of existing and proposed MST/ST radar systems throughout the world is given in Table 1, and their locations are noted on the world map in Fig. 2. Pertinent parameters for each system have been included for reference. The average power-aperture product has been obtained from published literature. For the phased dipole arrays, the antenna aperture is assumed to be comparable to the physical area. For other antenna configurations, the aperture is computed from the published antenna beamwidths. Antenna and transmission line losses are thereby neglected.

A number of the more sensitive systems – Jicamarca, Arecibo, Chatanika, Millstone, and EISCAT – have been designed as thermal (incoherent) scatter radars

Table 1

Parameters for some coherent pulsed radar systems involved in clear air studies

Facility	Location	Frequency, (MHz)	Wavelength, (m)	Average Power Aperture (W m²)	Beam Width, (deg)	Antenna Configuration
Jicamarca	Peru	49.9	6.01	2.0×10^{10}	1.0	Phased dipole array
Arecibo	Puerto Rico	430	0.70	8.7×10^{9}	0.17	Fixed dish/steerable feed
Poker Flat*)	Alaska	49.9	6.01	5.1×10^{9}	1.5	Phased dipole array
EISCAT*) (VHF)	N. Scandinavia	224	1.34	3.3×10^{9}	1.9×0.58	Steerable parabolic cylinder
Arecibo S-Band	Puerto Rico	2380	0.13	2.0×10^{9}	≃0.25	Steerable dish/Steerable feed
MU†)	Japan	48	6.25	5.0×10^{8}	3	Phased dipole array
Urbana	Illinois	40.9	7.33	4.4×10^{8}	3.6×4.8	Phased dipole array
EISCAT*) (UHF)	N. Scandinavia	933.5	0.32	2.4×10^{8}	≃0.6	Multistatic
Altair (VHF)	Kwajalein	155	1.94	1.8×10^{8}	2.8	Steerable dish
Altair (UHF)	Kwajalein	415	0.72	1.6×10^{8}	1.09	Steerable dish
SOUSY	Germany	53.5	5.61	7.6×10^{7}	5	Phased yagi array
Chatanika	Alaska	1290	0.23	5.8×10^{7}	0.6	Steerable dish
Millstone	Massachusetts	1290	0.23	5.8×10^{7}	0.6	Steerable dish
Sunset	Colorado	40.5	7.41	9.4×10^{6}	5×9	Phased dipole array
Platteville	Colorado	49.9	6.01	4.5×10^{6}	3×3	Phased dipole array
Wallops	Virginia	430	0.70	3.4×10^{6}	2.9	Steerable dish
Defford	England	2815	0.107	3.5×10^{5}	0.33	Steerable dish
NSSL	Oklahoma	2851	0.105	6.5×10^{4}	0.8	Steerable dish

*) Under construction.
†) Proposed.

Figure 3
The 50 MHz Jicamarca radar located near Lima, Peru.

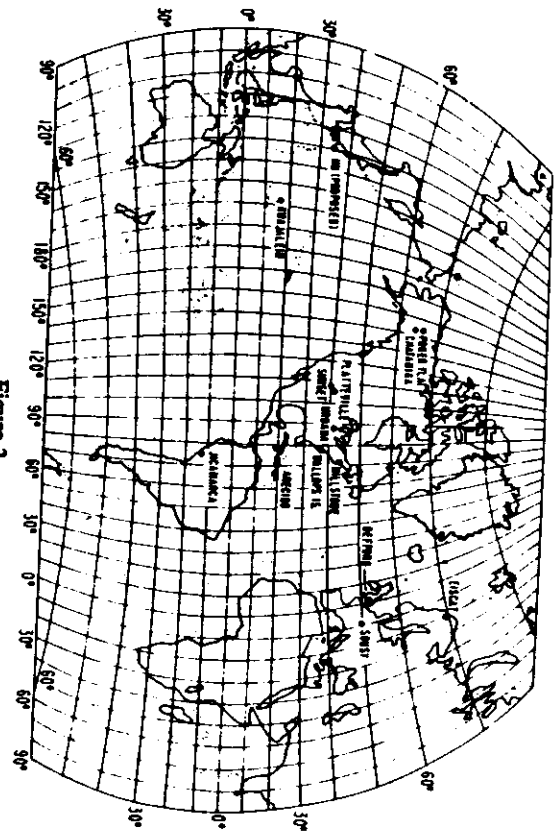

Figure 2
Location of various radar facilities with MST/ST capability listed in Table 1.

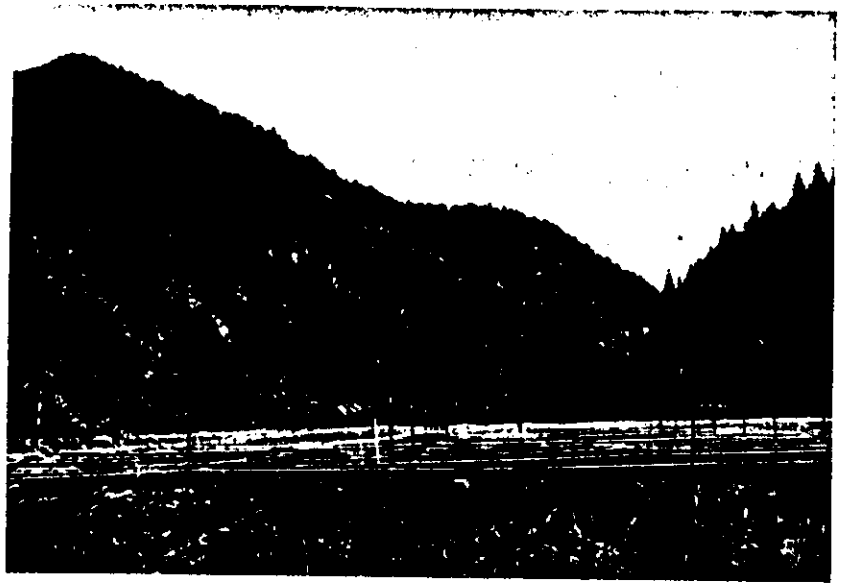

Figure 4
The 40 MHz Sunset radar located near Boulder, Colorado.

for ionospheric investigations. A similar number – SOUSY, Sunset, Platteville, Poker Flat, Urbana, Defford and the Japanese (MU) radar – have been or are being designed specifically as MST or ST radars.

The wide range of possible operating frequencies of MST/ST radars, particularly of the ST radars, allows for a variety of different antenna configurations. At the lower VHF frequencies it is possible to construct inexpensive dipole arrays having moderate steerability and large apertures. The Jicamarca array shown in Fig. 3 and the Sunset array shown in Fig. 4 are examples of this type of construction. A basic difference between these two systems is that, while the Jicamarca array consists of dipoles constructed of coaxial aluminum tubing, the Sunset array (and Platteville and Poker Flat) comprises collinear dipole arrays constructed from ordinary coaxial-cable (BALSLEY and ECKLUND, 1972). Antennas at higher frequencies range from the small but completely steerable dish at Chatanika (Fig. 5) to the large fixed dish at Arecibo (Fig. 6). Although a dish configuration is much more expensive than the dipole array, this disadvantage is largely offset by its inherent versatility.

c. Pertinent radar equations

The radar equation relates the received signal strength P_r to the radar parameters appropriate to any particular system and the volume reflectivity η, or reflection coefficient $|\rho|$, for any particular atmospheric process being studied. Although radar equations differ slightly for dishes and arrays, they can be treated in a unified manner. The pertinent radar equation for Fresnel reflection takes a somewhat different form.

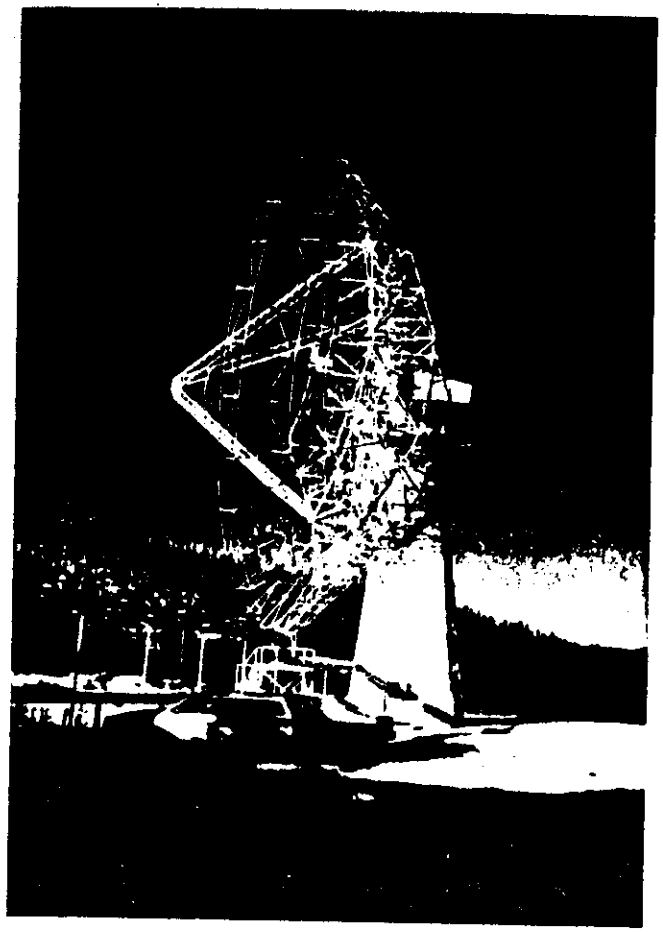

Figure 5
The 1290 MHz Chatanika radar located near Fairbanks, Alaska.

For scattering from distributed (beam-filling) targets the radar equation for dish antennas has been derived by PROBERT-JONES (1962). The radar equation for an array is given by VANZANDT *et al.* (1978). These equations can be expressed in the common form

$$P_r = \frac{\alpha^2 P_t A_e \Delta r}{9\pi r^2}\,\eta \qquad (1)$$

where α takes into account the efficiency of the antenna and waveguides, P_t is the peak transmitter power, $\Delta r\,(\equiv c\tau/2$, where τ is the pulse width) is the range resolution, r is the range and η is the volume reflectivity. For a dish $A_e\,(\simeq 2/3A)$ is the equivalent area of the antenna aperture having a physical area A. For an array $A_e = A\cos\chi$ where A is the physical area of the horizontal array and χ is the zenith angle. The

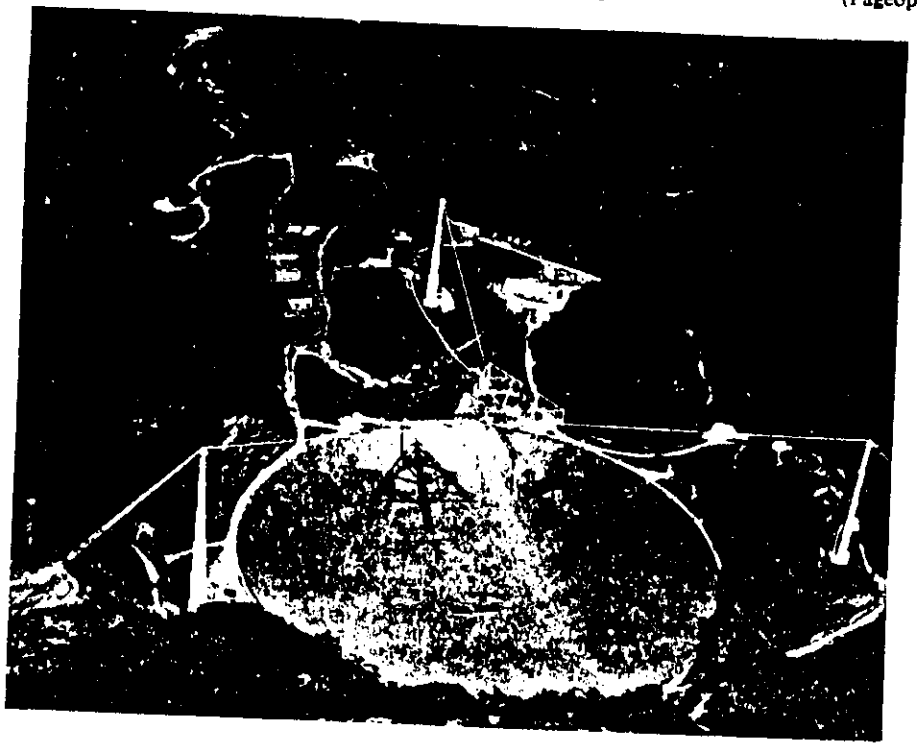

Figure 6
The 430 MHz Arecibo radar located near Arecibo, Puerto Rico.

$\cos\chi$ factor accounts for the apparent reduction in antenna area when the antenna is directed off-zenith.

For Fresnel reflection at vertical incidence from a horizontal layer assumed to extend over a Fresnel zone the appropriate radar equation has been derived by FRIEND (1949)

$$P_r = \frac{\alpha^2 P_t A_e^2}{4\lambda^2 r^2} |\rho|^2 \tag{2}$$

where $|\rho|^2$ is the power reflection coefficient and λ is radar wavelength.

d. Detectability and signal processing

The small radar scattering cross-section of the turbulent fluctuations, especially in the upper stratosphere and lower mesosphere, requires that MST systems have large power aperture products and employ relatively sophisticated signal detection and processing techniques. Most of the analysis procedures involve the power spectrum of the signal returns.

A typical power spectrum is shown in Fig. 7, where spectral power density is

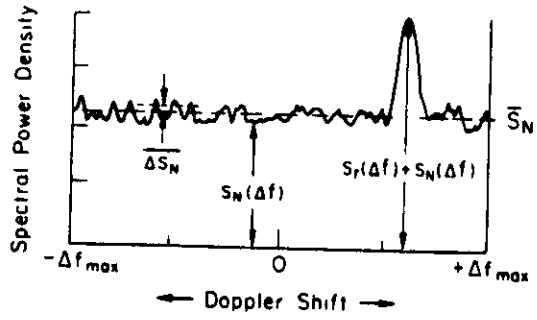

Figure 7
Example of a typical echo power spectrum from GAGE and BALSLEY (1978). See text for detai

plotted against Δf the Doppler shift of the transmitted frequency. The signal is inc cated by the enhanced peak in the region near the vertical arrow marked $S_r(\Delta f)$ · $S_N(\Delta f)$. (S_r and S_N refer to the power spectral densities of the signal and nois respectively.) The noise power spectral density in the absence of a signal is shown a $S_N(\Delta f)$. The mean power spectral density $\overline{S}_N$ of the noise is indicated by the horizont dashed line, and the r.m.s. of the statistical fluctuation around the mean level, $\overline{\Delta S_N}$ is also shown. The $\pm\Delta f_{max}$ limits are determined by the transmitted pulse rate an the number of coherent integrations. (Coherent integration involves the coheren summing of a number of samples obtained from a specific echoing volume afte sequential transmitter pulses and prior to performing a spectral analysis. Within limits, this process reduces the number of subsequent computer operations necessar to obtain the average echo power spectrum for a given period.)

GAGE and BALSLEY (1978) define the detectability of the received signal in term of $\overline{S}_r$ (the expected amplitude of the spectral peak of the received signal density after averaging) relative to $\overline{\Delta S_N}$ (the noise fluctuation level after averaging). Then, in terms of the radar equation for distributed targets (i.e., when the sampled volume is filled with scatterers), the detectability criterion may be written as:

$$\frac{\overline{S}_r}{\overline{\Delta S_N}} \simeq \frac{\overline{P}_t A_e F_1 F_2 \Delta r \eta \alpha^2 \sqrt{n_1}}{8\pi\sqrt{2} r^2 k (T_s + \alpha T_c)\, \delta f} \tag{3}$$

where $\overline{P}_t$ = average transmitter power, A_e = effective antenna area, F_1 = fractional received power passing through the receiver filter, F_2 = fractional received power passing through the coherent integration process, n_1 = number of power spectra averaged together to reduce the noise fluctuation, k = Boltzmann's constant ($= 1.38 \times 10^{-23}$ Joules/°K), T_s = system noise temperature, T_c = cosmic noise temperature at the antenna terminals, and δf = signal bandwidth (the halfwidth of the signal in Fig. 7). A discussion of the frequency dependent terms in (3) appears in GAGE and BALSLEY (1978).

Typical MST radar operation requires observations of the

a height resolution equal to or better than 1–2 km. This requirement limits the useful transmitter duty factor (on time/off time) to a few percent. Considerably better height resolution with no reduction in the average transmitted power can be achieved by phase coding the transmitter pulse (i.e., switching the phase of the transmitted signal at prescribed intervals within the transmitted pulse) and by appropriately decoding the received signal. Since the average power is not reduced, the resulting loss in detectability for distributed targets is only proportional to the effective pulse width decrease, and not to the square of the decrease that would result from the additional decrease in average transmitted power from a non-coded pulse. For layered targets, where the layer thickness is $\lesssim$ the pulse width, there will be no loss.

Of the number of phase-coding schemes in current use, the best choice appears to be the so-called complementary code (see, for example, CZECHOWSKY *et al.*, 1979). In this scheme alternate transmitter pulses are phase coded so that the sum of the autocorrelation functions of the two pulses (and the resulting echoes) for a single target produces a non-zero result at zero lag and a zero result at all other lags. This feature strongly reduces the effect of unwanted signal returns in nearby range gates, an important factor when the echo strength in nearby range gates can vary by more than an order of magnitude.

3. *Scattering and reflection mechanisms*

The echoing mechanisms (turbulent scatter, Fresnel reflection, and thermal scatter) which give rise to the signals observed on MST radars are somewhat diverse. Until recently these mechanisms have been studied in isolation. Indeed, radar studies of the clear neutral lower atmosphere and radar studies of the ionosphere have been quite separate disciplines. With the advent of the MST technique both disciplines are being brought together. In order to foster a better appreciation for the theoretical unity underlying these fields, we briefly survey in this section some of the theoretical foundations common to the study of radar echoes from the neutral and ionized atmosphere.

Basically, all radar echoes arise from scattering or reflection from inhomogeneities in the atmospheric dielectric constant ϵ or index of refraction n (FRIEND, 1949; BOOKER and GORDON, 1950; WOODMAN and GUILLÉN, 1974). The dielectric constant of free space is ϵ_0 ($= 10^{-9}/36\pi$ farads m^{-1}) and a relative dielectric constant can be defined by

$$\epsilon_r \equiv \frac{\epsilon}{\epsilon_0}. \tag{4}$$

The refractive index n is related to the dielectric constant by

$$n = \sqrt{\mu_r \epsilon_r} \tag{5}$$

where the relative permeability μ_r of air is approximately unity (BEAN and DUTTON, 1968).

The radio index of refraction is given approximately by

$$n - 1 = \frac{3.73 \times 10^{-1} e}{T^2} + \frac{77.6 \times 10^{-6} P}{T} - \frac{N_e}{2N_c} \tag{6}$$

where P is atmospheric pressure in mb, e is the partial pressure of water vapor in mb, T s absolute temperature, N_e is the number density of electrons and, for a critical frequency f. $N_c = 1.24 \times 10^{-2} f^2$ is the critical plasma density in MKS units (see, for example, YEH and LIU, 1972). Contributions to the atmospheric refractive index due to both bound and free electrons are contained on the r.h.s. of equation (6). The first two terms express the contributions due to bound electrons inherent in density fluctuations of water vapor and dry air, respectively, whereas the third term expresses the contribution due to the presence of free electrons. The first term is usually more important in the lower troposphere because of the high humidity. The second term, the dry contribution, is most important from mid-troposphere up to the stratopause ($\sim$50 km). The N_e/N_c ratio in the third term, which is usually negligible below 50 km. becomes the major contributing factor above this level where the electron density increases rapidly with height.

a. *Turbulent scatter*

The mechanism of turbulent scatter was invoked by BOOKER and GORDON (1950) to explain over-the-horizon tropospheric radio propagation. Since then the theory has been developed extensively (TATARSKII, 1971) and its relevance to tropospheric radio propagation has been established experimentally (CHISHOLM *et al.*, 1955; GJESSING, 1964; LANE and SOLLUM, 1965). With the advent of radar studies of the clear neutral atmosphere the theory has been tested more extensively and it has been established (HARDY *et al.*, 1966; KROPFLI *et al.*, 1968; LANE, 1969) that scattering from turbulent irregularities is the primary cause of clear air echoes observed at microwave frequencies (wavelengths $\sim$10 cm). The turbulent scattering theory has also been applied to lower-ionospheric radio propagation mechanisms (WHEELON, 1960). Several MST radar experiments in recent years (WOODMAN and GUILLÉN, 1974; RASTOGI and WOODMAN, 1974; RASTOGI and BOWHILL, 1976a,b,c; MILLER *et al.*, 1978; VANZANDT *et al.*, 1978; FUKAO *et al.*, 1978, 1979; and ECKLUND *et al.*, 1979) have established the relevance of turbulent scatter to explain some of the stronger echoes received at VHF throughout the middle atmosphere.

In evaluating the relevance of turbulent scattering for a particular radar frequency and for a specific atmospheric region, there are several parameters that must be considered. These parameters include the eddy dissipation rate (per unit mass) ϵ_d, which is proportional to the intensity of turbulence, and the outer scale L_0 and inner scale l_0 ($\equiv \nu^3/\epsilon_d)^{1/4}$, where ν is kinematic viscosity) of turbulence (see, for example,

TATARSKII, 1971). According to theory the radar backscattered signal arises from irregularities in the refractive index of length scale equal to one-half the radar wavelength. Therefore, for turbulent backscatter $\lambda/2$ should fall in the range $\lambda_{min} < \lambda/2 < \lambda_{max}$ where λ_{min} and λ_{max} are related to l_0 and L_0, respectively. Although some authors state this relationship rather loosely as $l_0 \ll \lambda/2 \ll L_0$, it is more precise to specify $C_1 2\pi l_0 < \lambda/2 < C_2 2\pi L_0$ where C_1 and C_2 are constants of order unity. MEGAW (1957) has determined $C_1 \approx 0.94$ and $C_2 \approx 0.75$. Note that L_0 is significantly smaller than the thickness scale of a turbulent layer.

Using values of ν from the standard atmosphere and typical values of ϵ_d expected for different altitudes we have constructed Fig. 8. The solid curve gives a rough variation with altitude of the minimum scale of turbulence λ_{min} ($\equiv 5.92 l_0$). Since $\lambda_{min} \propto \epsilon_d^{-1/4}$, it is insensitive to changes in ϵ_d. The shaded region in Fig. 8 illustrates the variation in λ_{min} due to an order of magnitude increase or decrease of ϵ_d. It should be noted that an increase in ϵ_d leads to a decrease in λ_{min}. Since the values of ϵ_d used in Fig. 8 are typical values and since ϵ_d can be expected to be several orders of magnitude larger in a region of locally intense turbulence, the maximum altitude to which a given radar can observe turbulence is likely to change from time to time.

The outer scale of turbulence is also dependent upon the intensity of turbulence. In the free atmosphere the outer scale is thought to be on the order of 10 m (VANZANDT *et al.*, 1978). In the lower ionosphere, WOODMAN and GUILLÉN (1974) and CUNNOLD (1975) argue that a thickness scale is about 100 m.

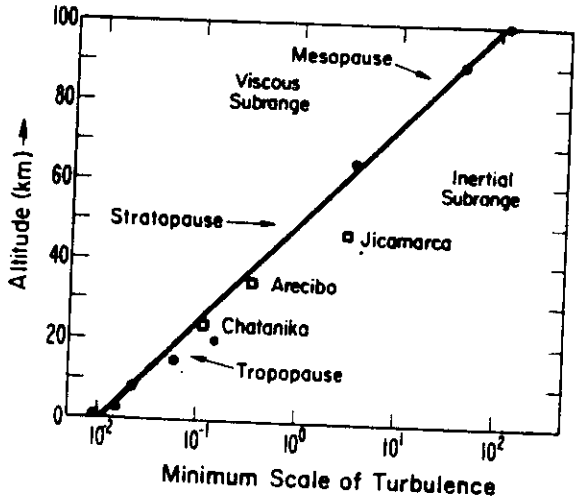

Figure 8

Height distribution of the minimum scale of turbulence (solid circles) ($m/2\pi$ radians) based on data from RASTOGI and BOWHILL (1967c); CUNNOLD (1975); ROPER (1977); and GAGE *et al.* (1979). The open squares denote the maximum height of observed atmospheric echoes (non-ionized region) for sensitive radars operating at three different frequencies.

The general expression for reflectivity for backscattering due to turbulence scattering is given by (TATARSKII, 1971)

$$\eta_{turb} = \frac{\pi^2}{2} K^4 \Phi_n(K) \tag{7}$$

where K is the wavenumber ($=4\pi/\lambda$) of disturbances to which the radar is sensitive and $\Phi_n(K)$ is the three-dimensional wavenumber spectral density for refractive index fluctuations. For locally homogeneous and isotropic inertial range turbulence

$$\Phi_n(k) = 0.033 C_n^2 k^{-11/3} \tag{8}$$

where $k = 2\pi/\lambda$. The refractivity structure constant C_n^2 is related to the mean-square fluctuations $\overline{(\Delta n)^2}$ of radio index of refraction by

$$C_n^2 = 5.45 \overline{(\Delta n)^2} L_0^{-2/3}. \tag{9}$$

By substitution of equation (8) into equation (7) we find

$$\eta_{turb} = 0.38 C_n^2 \lambda^{-1/3} \tag{10}$$

and using equation (9)

$$\eta_{turb} = 2.07 \overline{(\Delta n)^2} L_0^{-2/3} \lambda^{-1/3}. \tag{11}$$

For a detailed derivation of these results see HARDY *et al.* (1966).

It is instructive to examine the above relationship in terms of the mean square electron density fluctuation $\overline{(\Delta N_e)^2}$ for mesospheric applications. WOODMAN and GUILLÉN (1974) show

$$(\Delta n)^2 = \left[\frac{f_p^2 \, \Delta N_e}{2 f^2 N_e}\right]^2 \tag{12}$$

where f_p is related to the local electron density by $f_p = (80.65 N_e)^{1/2}$, and the transmitter frequency $f = c/\lambda$ where c is the velocity of light in vacuo. Combining equations (11) and (12),

$$\eta_{turb} = 3.25 \times 10^3 \overline{(\Delta N_e)^2} c^{-4} L_0^{-2/3} \lambda^{11/3} \tag{13}$$

where a strong wavelength dependence of the volume reflectivity is indicated.

b. Fresnel (partial) reflection

Fresnel reflections (also termed partial or specular reflections) from coherent structure and sharp gradients have long been thought to play an important role in long distance radio propagation. As with turbulent scatter, this mechanism appears to contribute to radar echoes both from the lower neutral atmosphere and the ionosphere, especially at vertical incidence for long wavelength radars. In the

ionosphere partial reflection sounding has a long history starting in the early 1950s. Most experiments have been made in the frequency range 1–5 MHz. This work has been reviewed by BELROSE (1970) and more recent developments are surveyed by EVANS (1974). Recent work in the lower neutral atmosphere with VHF radars has offered considerable evidence for the importance of Fresnel reflections from stable, horizontally-layered structure in the troposphere and stratosphere (GAGE and GREEN, 1978; RÖTTGER and LIU, 1978; FUKAO *et al.*, 1978; RÖTTGER and VINCENT, 1978) and in the mesosphere (FUKAO *et al.*, 1979).

The general form of the power reflection coefficient $|\rho|^2$ for an electromagnetic wave at vertical incidence upon an infinite horizontal layer is (e.g., WAIT, 1962)

$$|\rho|^2 = \frac{1}{4}\left|\int_{-l/2}^{+l/2} \frac{dn}{dz} \exp\left[-\frac{4\pi i z}{\lambda}\right] dz\right|^2 \tag{14}$$

$$= \frac{|\Delta n|^2}{4}\left|\int_{+l^*/2}^{-l^*/2} \frac{d(n/\Delta n)}{dz^*} \exp\left[-4\pi i z^*\right] dz^*\right|^2 \tag{15}$$

where z is altitude, l is the thickness of the layer, Δn is the total change of n across the layer, $l^* = l/\lambda$ and, $z^* = z/l$.

For some simple layer shapes the integral can be expressed in closed form. For a step of magnitude Δn

$$|\rho|^2 = |\Delta n|^2/4. \tag{16}$$

For the constant gradient,

$$|\rho|^2 = \frac{|\Delta n|^2}{16\pi^2}\left(\frac{\sin 2\pi l^*}{l^*}\right)^2. \tag{17}$$

For a smoothly varying layer of the form

$$n = n_0 + \Delta n\left[\frac{\exp 4z^*}{1 + \exp(4z^*)}\right] \tag{18}$$

the reflection coefficient is given by (FRIEND, 1949)

$$|\rho|^2 = \frac{|\Delta n|^2}{4}\left[\frac{9l^*}{\sinh(9l^*)}\right]^2. \tag{19}$$

The oscillations in equation (17) are the result of interference caused by the discontinuities in dn/dz. Variation of $|\rho|^2$ as an inverse power of l^* is typical. The approximate expressions used by SAXTON *et al.* (1964) and GAGE and GREEN (1978) are intended for estimation of $|\rho|^2$ to an order of magnitude in the absence of detailed knowledge of the shape of layers of refractive index.

c. *Thermal (incoherent) scatter*

Several of the large radars listed in Table 1 have been used for the past two decades to observe the weak scattering from random thermal motion of electrons. The subject

of thermal scattering has been reviewed by EVANS (1969, 1974). Most of the research in this field has been limited to altitudes above 80 km and will not be considered here. Recently, however, thermal scatter has been observed down to 65 km at Arecibo (HARPER, 1978), and to even lower heights at Chatanika (HUNSUCKER, 1974; REAGAN and WATT, 1976) under disturbed conditions.

The volume reflectivity for thermal scattering is, with some simplification,

$$\eta_{t.s.} = N_e \sigma_e / 2 \tag{20}$$

where N_e is the number density of electrons and σ_e ($\approx 10^{-28}$ m^2) is the backscattering cross-section of an electron. The received power is proportional to the electron density, and the altitude profile of received power can be used to obtain the altitude profile of electron density.

Thermal scatter can be a useful technique for probing the ionized portion of the middle atmosphere, especially for radars operating at wavelengths less than one meter. At these wavelengths the turbulent echoes at mid stratospheric heights and higher will be suppressed, since the pertinent fluctuations are viscously damped. This allows measurement of the background electron density, a necessary parameter in assessing the relative contributions of the turbulent fluctuations. Also, since the electrons and neutral particles are strongly coupled below about 90 km, the Doppler shifted echoes provide a measurement of the neutral wind.

d. *General comments on MST scattering and reflection mechanisms*

In the above discussion we have considered a number of scattering and reflection mechanisms appropriate to MST radar studies. The relative importance of each mechanism is assessed in the following paragraphs.

It is clear that turbulent scatter (including turbulent scatter enhanced by free electrons) holds the dominant role for continuously measuring winds, waves, and turbulence at all heights. The major limitations of turbulent scatter at VHF and UHF are that (1) typically the electron-density-enhanced scatter from the mesosphere is possible only during the daytime, and (2) in the upper stratosphere and mesosphere, turbulent echoes may not be continuous on spatial scales less than a few hundred meters. However, except for determining the diurnal variations of mesospheric turbulence and winds or for the examination of fine scale vertical structure of atmospheric parameters, these limitations do not appear to be of major importance.

Comparison between Fresnel reflection echo amplitudes and turbulent scatter echo amplitudes appears to offer an excellent means of studying atmospheric stability at all heights and of possibly extending the maximum height range of VHF ST systems. It is worthwhile pointing out that the possibility of Fresnel-like reflections at off-vertical angles from large refractive index structures has been considered (METCALF and ATLAS, 1973). This may be the cause of the strongly varying off-vertical

echo amplitudes obtained on MST/ST radars. This particular idea, however, is embrionic, and much remains to be done.

Thermal scatter is an additional useful adjunct that can be used to measure the background electron densities and the mesospheric winds during daytime without depending on the presence of neutral turbulence. Therefore, it enables sensitive radars operating at wavelengths smaller than the local minimum scale of turbulence to monitor the mesospheric wind field. However, studies of turbulence parameters are precluded at heights where the scattering scale size is smaller than the minimum scale of turbulence.

Scattering from meteor trails has the potential of extending mesospheric wind (and possibly turbulence) studies to nighttime periods. This mechanism which may be considered as a Fresnel reflection process (GROSSI *et al.*, 1972) yields useable data during daytime and nighttime from about 75 km to 100 km on radar systems with MST capability. Preliminary results at Poker Flat indicate that two orthogonal antenna directions can be used to determine the average mesospheric winds with good resolution (BALSLEY *et al.*, 1979).

4. *Stratospheric observations*

Enormous progress has been made during the past five years in observing the lower (neutral) atmosphere below 20 km using Doppler radar. In recent years many observations and experiments have documented the capabilities of Doppler radar for observing wind, waves, turbulence and even atmospheric stability. Many of the recent developments have been surveyed by GAGE and BALSLEY (1978). Here, we summarize the Doppler radar capabilities for observing the clear neutral atmosphere, focusing attention on those developments which are of special interest in studying the middle atmosphere.

Two types of radar echoes will be considered in this section. The first type is the echo received via turbulent scatter. These echoes provide a measurement of the radial component of the wind and the intensity of refractivity turbulence as a function of height. A time sequence of such measurements enables the observation of atmospheric motions over a wide range of periods and heights. The second type of echo arises from Fresnel reflections when the radar antenna is directed vertically. The intensity of these reflections has been shown to be well correlated with atmospheric stability. Experiments to date indicate that these echoes are much stronger at longer wavelengths; their presence constitutes a new dimension in radar probing for VHF radars.

a. Winds

Figure 9 shows a typical set of normalized Doppler spectra vs. height for the Platteville radar produced from observations taken on the north antenna on 7 February 1979 in the presence of a moderate jet stream. The radial velocity scale is

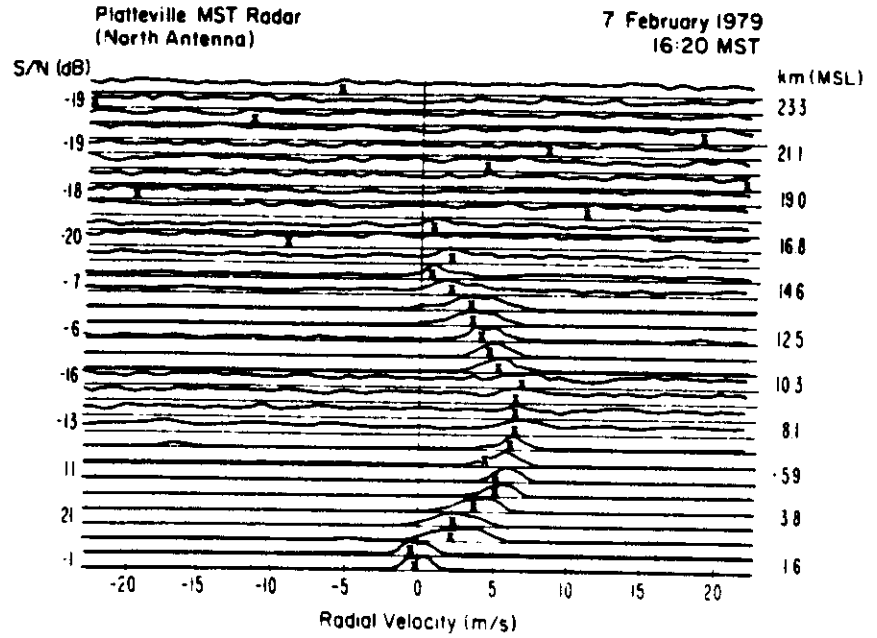

Figure 9
Normalized echo power spectra versus height at 725 m intervals obtained from the prototype MST radar at Platteville, Colorado. Signal-to-noise ratios shown on the left for every third height. The X's denote the computer-estimated mean spectral shift (scaled here in radial velocity). For $S/N \leq -17$ dB, the X's represent the mean spectral shift of the noise level in the absence of signal and should be ignored.

proportional to the Doppler frequency shift and the mean shift of each spectrum is approximately the mean radial wind velocity in the radar-observed volume. For the 15° antenna zenith angle the horizontal wind velocity is about a factor of four larger than its projection along the antenna beam. This example shows the profile of the southward wind with a maximum southward velocity close to 30 m/s.

Vertical profiles of the radar-observed horizontal winds have been compared with vertical profiles of horizontal winds deduced from balloon sounding techniques for several of the radars considered here. As might be expected, the quality of the agreement is best for nearly simultaneous, nearby observations. The agreement deteriorates somewhat over rough terrain where temporal and spatial variability of the wind is large.

A profile of wind speed and direction observed by the Arecibo radar (FARLEY *et al.*, 1979) is presented in Fig. 10. This profile, extending in altitude to above 20 km, was obtained from analyzing VAD (Velocity Azimuth Display) data as a function of height. Also shown is the wind profile obtained nearly simultaneously by the NWS (National Weather Service) rawinsonde launched from San Juan, PR (about 70 km east of Arecibo). Taking this separation into account, the agreement is excellent.

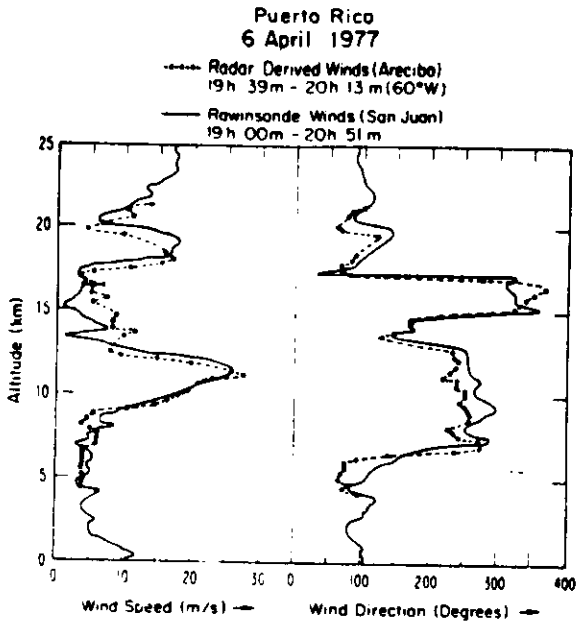

Figure 10
Comparison of vertical profiles of wind speed and direction observed by Arecibo radar on 6 April 1977 with nearly simultaneous NWS rawinsonde observation from San Juan, Puerto Rico. (After FARLEY *et al.*, 1979.)

Additional profiles from Chatanika and Arecibo (which both use relatively expensive dish antennas) show excellent agreement when compared with routine balloon wind observations. Although not included herein, similar comparisons made with the Sunset radar (GREEN *et al.*, 1979), the temporary Poker Flat radar (ECKLUND *et al.*, 1977), and the Platteville radar (ECKLUND *et al.*, 1979) demonstrate that at longer wavelengths the less expensive radars employing phased arrays can obtain equally accurate wind profiles.

Continuous – or essentially continuous – radar wind observations are very useful for the study of mesoscale variations in the atmospheric wind field. Figure 11 (from ECKLUND *et al.*, 1979) shows a sequence of hourly averaged wind profiles observed over a 48-hour period using the prototype MST radar at Platteville. Times of synoptic rawinsonde observations are indicated by darkened profiles. Clearly, much of the variability in the wind field was missed by the twice daily synoptic soundings. Similarly, a set of observations by the Sunset radar of a jet stream passage on 15–16 April 1976, has been analyzed (GREEN *et al.*, 1978) to yield a time height cross-section of vertical and horizontal winds over the radar site.

The variability of the mesoscale wind can be determined simultaneously at many altitudes using the time series of wind observations available from long observing periods. GAGE and CLARK (1978) have analyzed the variability of the jet stream winds

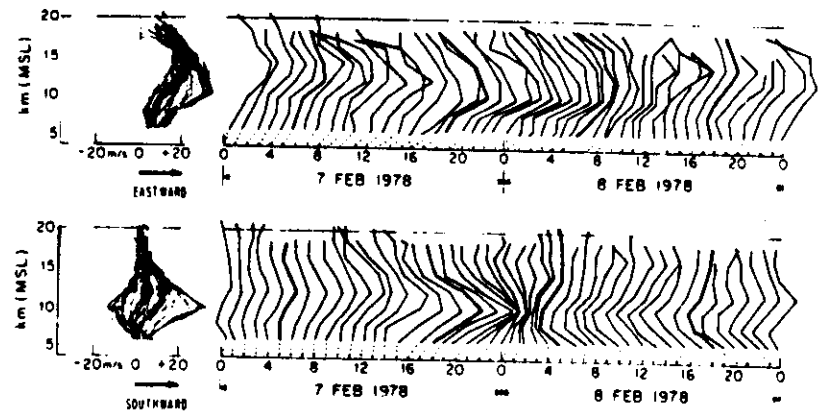

Figure 11
Hourly averaged wind profiles observed by the Platteville, Colorado radar. The darkened profiles at 05 hr and 17 hr correspond to times of synoptic rawinsonde observations at Denver. (After ECKLUND *et al.*, 1979.)

observed by the Sunset radar over a 14-hour period on 15–16 April 1976. Although a systematic height variation was found in the power law for lag variability ($\sigma_v \equiv \overline{[v(t) - v(t-\tau)]^2}$, where v is velocity and τ is time lag) over lags τ ranging from a few minutes to several hours, the average variability for all heights combined, satisfies a $\tau^{1/3}$ power law. If the temporal variability follows the 1/3 power law out to lag times of several hours during such large winds, spatial variabilities on scales of several hundred kilometers must also be consistent with the same power law. Since a 1/3 power law for lag variability is consistent with $k^{-5/3}$ inertial range (GAGE, 1979) these observations provide evidence for a mesoscale inertial range. Because turbulence cannot be three-dimensionally isotropic on these scales, this is probably a two-dimensional $k^{-5/3}$ inertial range (KRAICHNAN, 1967; GAGE, 1979).

The vertical wind component can be determined from the Doppler shift of the echoes from turbulent irregularities. Vertical velocities can be inferred from a VAD (Velocity Azimuth Display) or from a vertical scan at one azimuth. Vertical velocities derived from these methods are subject to errors arising from horizontal gradients of the wind, etc. (BALSLEY *et al.*, 1977). A more direct method is to measure the vertical velocity using a vertically-directed radar beam. This latter method suffers from the problem of differentiating the spectrum of the slow vertical motions from that of stationary terrain echoes arriving via the antenna sidelobes. Vertical profiles of the vertical velocity obtained sequentially during a two-hour period by all three methods at Chatanika (PETERSON and BALSLEY, 1980) are reproduced in Fig. 12. With some exceptions, these measurements show the same approximate magnitude

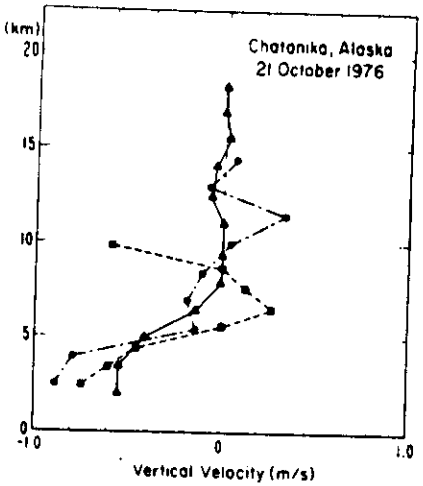

Figure 12
Vertical profiles of the vertical wind inferred from Chatanika radar data (PETERSON and BALSLEY, 1980). The dashed lines refer to azimuth-scan data (VAD), dashed-dotted lines to elevation-scan data, and the solid line to data obtained with the antenna directed vertically.

of the vertical velocity. Of the three methods, the most accurate is to directly measure the vertical velocity with a vertically directed beam. It is important to realize that these results provide local measurements of the vertical velocity – in this case the vertical velocity was probably associated with a lee wave – and it is not surprising that the magnitude of the velocities so obtained are considerably greater than the 'mean' synoptic scale vertical velocities derived indirectly from routine rawinsonde data.

b. Waves

Any technique that can be used to continuously measure wind or other atmospheric variables at many heights is ideal for observing atmospheric waves. Atmospheric waves of periods ranging from seconds to days have been observed using MST/ST radars. Here we illustrate the kinds of observations that can be made by selecting examples of each type of wave motion that has been observed to date.

On the shortest time scale, the microbarom is a very short period infrasonic wave of period close to 5 seconds (DONN and RIND, 1972). Microbaroms are thought to be generated by ocean waves and travel to great distances in the atmosphere. They are associated with pressure amplitude variations of a few microbars and have been studied primarily by sensitive ground-based pressure sensing devices. Preliminary data showing relatively continuous short period ($\simeq 4$ s) intensity fluctuations in back-scattered power have been observed using the Jicamarca radar (LAGOS, private communication). These fluctuations are seen at tropospheric-stratospheric heights,

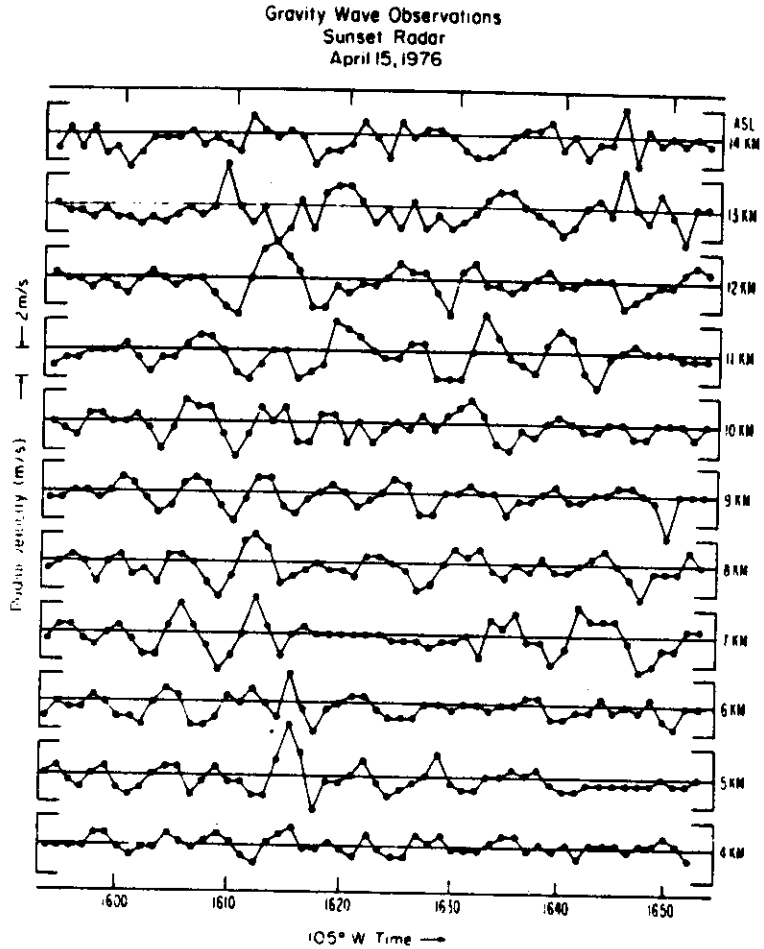

Figure 13
Fluctuations in the detrended radial velocity due to gravity waves observed on the north-directed antenna of the Sunset radar on 15 April 1976. (GREEN and VANZANDT, private communication, 1978; see also VANZANDT *et al.*, 1979.)

are coherent over a few km in height, and the fluctuation intensity appears to be quite anisotropic with respect to antenna azimuth. It has not been possible to isolate the mechanism whereby microbaroms would modulate the normal echoes and clearly much more research will be required to understand this phenomenon.

Internal gravity waves of a few minutes period have been observed in the troposphere by the Sunset radar (VANZANDT *et al.*, 1979) and in the lower stratosphere by the Jicamarca radar (RÜSTER *et al.*, 1978). Figure 13 shows gravity waves observed during the passage of a jet stream over Sunset radar on 15 April 1976. The observed

wave properties are in good agreement with theoretical calculations (GRANT, 1979; VANZANDT *et al.*, 1979) which show that the waves are generated in a region of high shear near 7 km. Gravity waves of longer periods (a few hours) are also evicent in the jet stream observations but have not yet been studied extensively.

Waves of tidal period have been observed recently (FUKAO *et al.*, 1978) at stratospheric altitudes at Jicamarca. The quasi-vertical wind (obtained from a 1.06° wide antenna beam at a zenith angle of 0.36°) observed at Jicamarca during a 24 h period spanning 23–24 May is shown for several stratospheric altitudes in Fig. 14. Although these data are contaminated by horizontal winds (causing the non-zero means), they show evidence of tidal oscillations in the true vertical velocity on the order of 1–2 cm/s. Zonal winds observed in the same experiment showed a very large diurnal component of amplitude of 1–5 m/s.

Planetary waves are easily observed as they propagate past an MST radar. Figure 15 shows the oscillations in the meridional component of the wind due to travelling Rossby waves observed by the Platteville radar (ECKLUND *et al.*, 1979) during the seven day period 7–14 February 1978. These waves are most evident in the large synoptic-scale structure of jet stream winds. Their maximum amplitude is of the order of 50 m/s and their observed periods range from about a day to many days. In accordance with the Rossby wave dispersion relation, the short wavelength Rossby waves propagate most rapidly from west to east while the largest scale waves may be stationary or even propagate westward.

c. *Turbulence*

There are several ways in which quantitative measurements of turbulence can be deduced from clear air radar observations. These include estimates from (1) the mean refractivity turbulence structure constant $\overline{C_n^2}$ observed in the radar volume, (2) the width of the observed Doppler spectrum, and (3) time series analysis of observed mean winds.

According to theory, the volume reflectivity from clear air echoes is proportional to the refractivity turbulence structure constant C_n^2, provided the radar half-wavelength lies within the inertial subrange. For stationary turbulence C_n^2 is defined by

$$\overline{[n(r_0 + r) - n(r_0)]^2} \equiv C_n^2 r^{2/3} \tag{21}$$

where n is the radio refractive index. It provides a measure of the intensity of refractivity turbulence in a manner analogous to the way in which ϵ_d provides a measure of the intensity of velocity turbulence.

The gross structure of turbulence in the free atmosphere is intermittent in time and inhomogeneous in space with active turbulence confined to thin horizontal layers. Within the turbulent layers the small-scale structure of turbulence approaches a locally homogeneous and isotropic condition and approximately conforms to inertial range turbulence theory. In view of the inhomogeneity of the gross structure it is

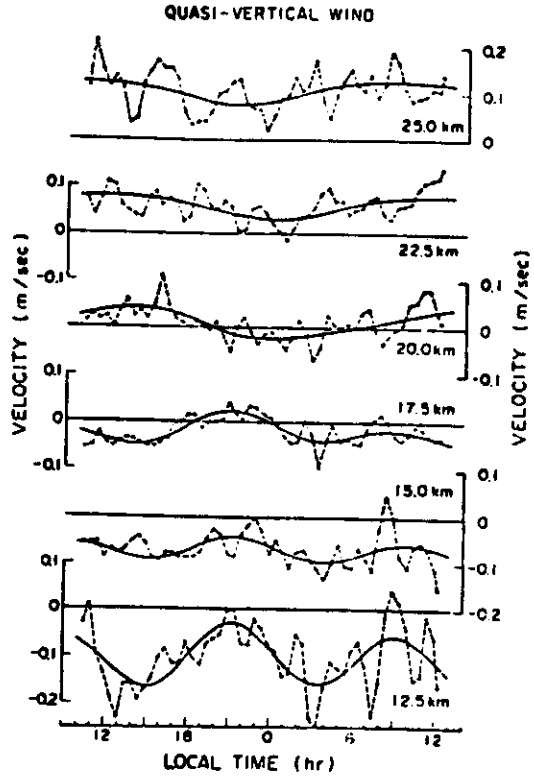

Figure 14
One-hour running means (broken lines) of quasi-vertical (upward) velocities at Jicamarca on 23–24 May 1974. Solid lines are the best fit combination of 24h and 12h sinusoids. (After FUKAO *et al.*, 1978.)

useful to distinguish between local and volume measures of turbulence. For example, the radar measures a volume-averaged $\overline{C_n^2}$ which is related to the local $(C_n^2)_{turb}$ by

$$\overline{C_n^2} = F \cdot (C_n^2)_{turb} \tag{22}$$

where F is the fraction of the observed volume which is turbulent (VANZANDT *et al.*, 1978).

A radar measurement of $\overline{C_n^2}$ can be obtained from the amplitude distribution of the Doppler spectra such as are shown in Fig. 9. Note that the peak amplitudes of the spectra in Fig. 9 are normalized. The actual integrated signal-to-noise ratio, S/N, is given at the left of each spectrum. Note, also, that the S/N values decrease by more than a factor of 10^4 from 3 to 17 km. The observed S/N can be expressed in terms of the volume reflectivity. Since the volume reflectivity is directly proportional to C_n^2, the vertical profile of received power with height can be converted to a vertical profile of C_n^2.

Radar observations of $\overline{C_n^2}$ sometimes show more than an order of magnitude

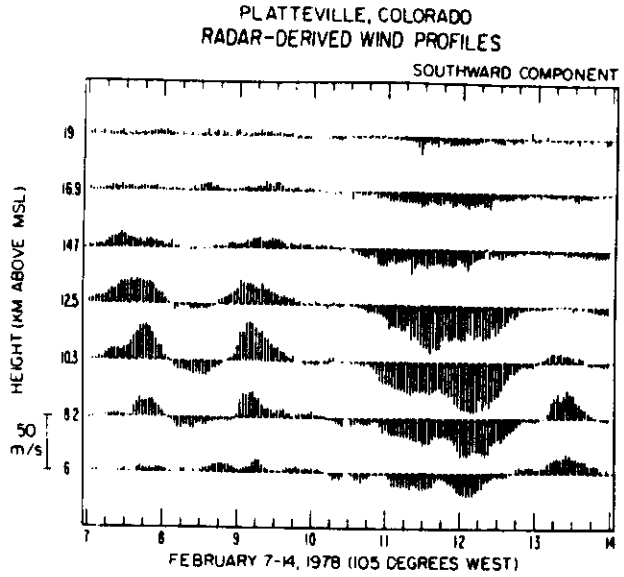

Figure 15
Hourly values of the meridional wind between 6–19 km during 7–14 February 1978 obtained with the Platteville radar. Southward values are plotted above the horizontal dashed line at each height and northward values are plotted below. Magnitude scale is on left. (After ECKLUND *et al.*, 1979.)

variation within minutes as shown in Fig. 16, over a few km altitude as shown in Fig. 17, and horizontally with spatial dimensions of a few km as shown in Fig. 18. Vertical profiles of observed $\overline{C_n^2}$ have proved especially useful in determining the meteorological factors responsible for the observed $\overline{C_n^2}$. VANZANDT *et al.* (1978) have had considerable success in parameterizing mean C_n^2 profiles using routine rawinsonde observations of wind, temperature and humidity. This has been accomplished despite

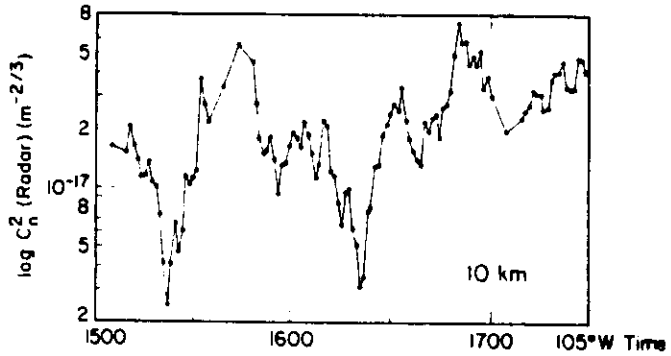

Figure 16
A time series of C_n^2 observed by the Sunset radar at 10 km on 15 April 1976. Height resolution is about 1 km. (After VANZANDT *et al.*, 1978.)

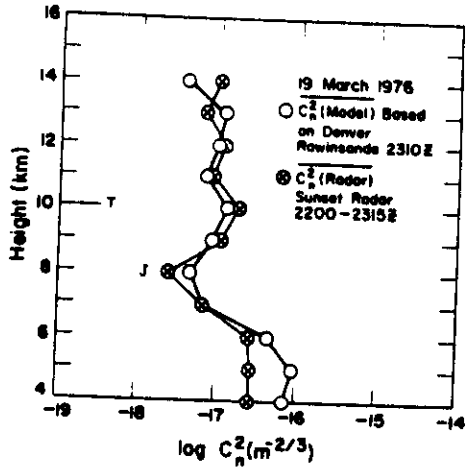

Figure 17
Comparison of the vertical profile of C_n^2 observed by the Sunset radar on 19 March 1976 with calculated values using a new theoretical model. *T* and *J* indicate the altitude of the tropopause and jet stream maximum velocity, respectively. (After VANZANDT *et al.*, 1978.)

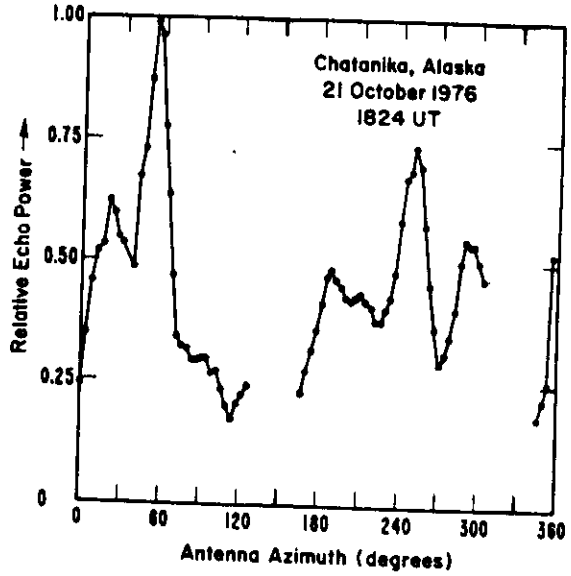

Figure 18
Spatial variation of relative echo power ($\propto C_n^2$) observed at a height of 12 km by the Chatanika radar. These data were obtained by observing the echo power at one range as the antenna rotated 360°. Shaded regions indicate antenna azimuths where the radial velocity is near zero, precluding accurate determination of echo power. (Similar to BALSLEY *et al.*, 1977.)

several assumptions and approximations in the analysis, the most severe of which is the use of a constant value of 10 m for L_0, the outer scale of turbulence. The theoretical model used by VanZandt *et al.* has been calibrated against radar observed mean C_n^2 profiles and comparisons have been presented for several MST/ST radars (Gage *et al.*, 1978). A sample comparison of observed and calculated vertical profiles of C_n^2 is shown in Fig. 17. This model, although still under development, shows considerable promise for the development of a climatology of C_n^2 from archival meteorological data. Such a climatology would have several applications, including guidance for designing new MST radars for different parts of the world.

The rate of dissipation per unit mass of turbulent kinetic energy ϵ_d is an important turbulence parameter. The relationship between C_n^2 and ϵ_d is discussed in some detail by Gage and Balsley (1978) and Gage *et al.* (1979). Recent developments have raised the possibility that under certain circumstances ϵ_d can be determined from radar observations of $\overline{C_n^2}$ alone.

The width of the Doppler spectrum may provide an independent measure of ϵ_d under suitable circumstances. The technique has been developed for use with microwave Doppler radars that are sensitive to hydrometeors. For such radars the observed Doppler spectral width is partly due to the variance of precipitation fall speeds so that special techniques have had to be developed to infer the spectral width of the turbulent component alone (Gorelick and Mel'nichuk, 1938; Frisch and Clifford, 1974). The determination of ϵ_d from clear air Doppler radars is inherently simpler, but still involves practical measurement difficulties. This aspect of the subject has also been considered in more detail by Gage and Balsley (1978).

The remaining technique for obtaining estimates of ϵ_d employs the familiar spectral, or time series, analysis of a sequence of wind observations. To obtain ϵ_d, the velocity spectrum of the velocity structure function is determined first. After demonstrating the inertial range dependence of the spectrum or structure function, known relationships between these quantities and ϵ_d can be used to deduce ϵ_d. For small-scale turbulence this technique has been used by Kropfli (1971) and Lilly *et al.* (1974) to determine ϵ_d from aircraft observations. Frisch and Strauch (1976) used this technique to determine ϵ_d from microwave Doppler radar observations during a convective storm. Ellsaesser (1969) also used this method to estimate ϵ_d for larger-scale motions, but there is still some controversy concerning the applicability of the theory to these larger scales of atmospheric motion.

d. Stability

Hydrostatic atmospheric stability is proportional to the potential temperature gradient. The potential temperature gradient is related to the gradient in absolute temperature T by

$$\frac{1}{\theta}\frac{\partial\theta}{\partial z} = \frac{1}{T}\left(\frac{\partial T}{\partial z} + \Gamma\right) \qquad (23)$$

where θ is the potential temperature and Γ is the adiabatic lapse rate of 9.8°C Hydrostatic stability plays a very important role in determining the dynamics of atmosphere. Very stable atmospheric regions suppress vertical motion and micro turbulence and permit the development of large vertical gradients of wind, hum pollutants, ozone, etc.

In Section 3b the theory for Fresnel reflection from stable atmospheric layer presented. Below, we review some of the recent observations by VHF radars demonstrate the existence of Fresnel reflection echoes from the troposphere stratosphere, reveal the close relationship between these echoes and atmosp stability, and show how the presence of these echoes can be used to determin height of the tropopause.

With the Sunset radar, it is often observed that the signal received on the ve antenna is considerably enhanced compared to the signal received on ante pointed 30° off the zenith (Gage and Green, 1978). This enhancement has attributed to Fresnel reflection from stable regions of the atmosphere. The enha intensity and the narrowed spectral width of the vertical returns appear to be dir related to the stability of the atmosphere. Similar observations have been using a bi-static radar (Gage *et al.*, 1973) and more recently using the monos SOUSY radar (Röttger and Liu, 1978) and the Jicamarca radar (Fukao *et* 1979; see Fig. 19).

A comparison of the vertical and oblique power profiles using the Sunset r

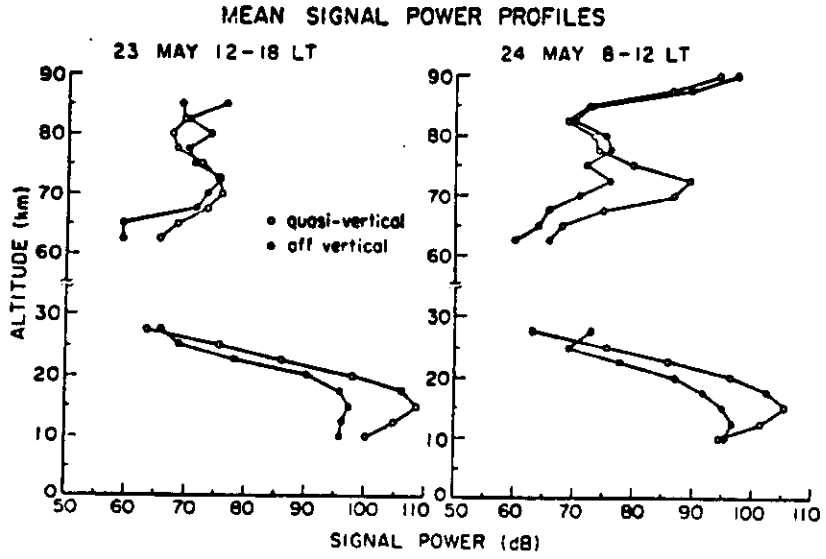

Figure 19
Mean signal power versus height in quasi-vertical (≃0.4° to southwest) and off-vertical (≃ to west) antennas observed at Jicamarca on 23–24 May 1974. (After Fukao *et al.*, 1979.

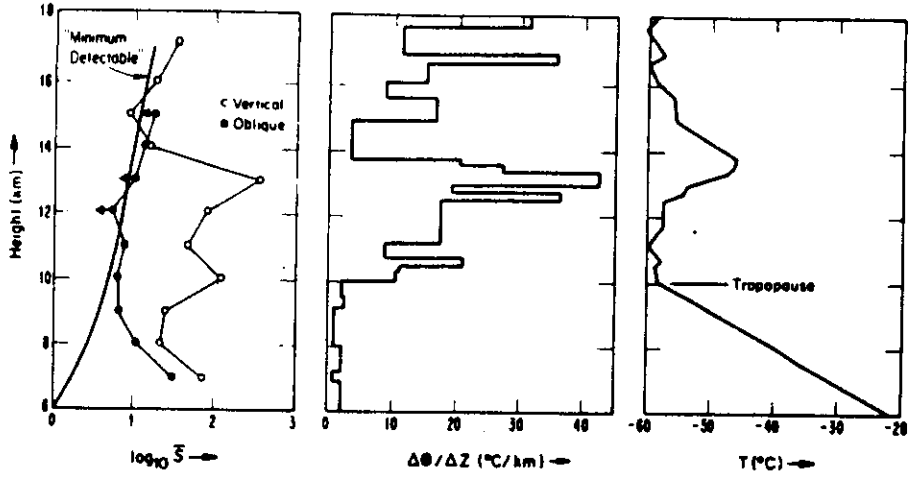

Figure 20
Vertical profiles of the normalized received signal observed by the Sunset radar near 0000 UT, 26 March 1977. Also shown are the vertical profile of potential temperature gradient and the vertical temperature profile from 0000 UT, 26 March 1977, Denver NWS sounding. (After GAGE and GREEN, 1978.)

on 26 March 1977 appears in Fig. 20. The vertical profile of the measured temperature and the inferred potential temperature gradient obtained from the nearly simultaneous Denver radiosonde are also shown in this figure. The radar power profiles have been normalized and range corrected to compensate for the r^{-2} range dependence. Note that the power profile at vertical incidence is correlated with the vertical profile of the potential temperature gradient (at least up to 14 km where the radar signal becomes very weak). Note in particular the increase in radar signal just above the tropopause at 10 km. Also, the strongest signal received on the vertical antenna is from the height of a very stable region near 13 km. Even though the details of the reflection mechanism are quite complex, the technique holds promise of a quantitative measure of atmospheric stability.

A very practical application of the enhanced Fresnel reflection echoes is the determination of the height of the tropopause. GAGE and GREEN (1979) have presented a comparison of tropopause heights in the vicinity of Denver, CO, as determined by the routine NWS Denver soundings and by the Sunset radar. The comparison reproduced in Fig. 21 covers the three month period March–May 1977. The tropopause during this period varied between 7 and 14 km and in almost all cases the radar tropopause was found to agree within the altitude increment of the one kilometer range gates.

The ability of VHF radars to observe Fresnel reflection echoes in stable regions of the atmosphere enables the longer wavelength ST radars to observe considerably higher into the stratosphere than would be possible using turbulent scatter alone. Although it may be possible to extract vertical velocities from the narrow specular

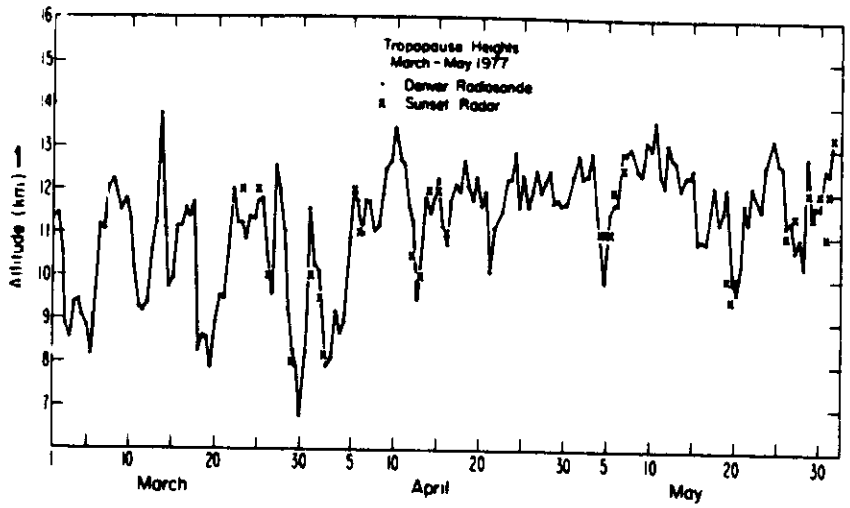

Figure 21
Sampled time series of the tropopause height determined from Denver radiosonde data for March 1977 and concurrent estimates of the tropopause height determined using the Sunset radar. (After GAGE and GREEN, 1979.)

echoes, echoes obtained from turbulent scattering at oblique incidence will still be needed for the measurement of horizontal velocities.

5. *Mesospheric observations*

a. *Thermal scatter*

As discussed earlier, although the MST technique presumes a non-thermal scattering process involving turbulence-generated refractive index fluctuations, radar returns via thermal (incoherent) scattering also yield useful data on the background electron density and the neutral wind field.

Mesospheric thermal scattering experiments at Arecibo have been reported by MATTHEWS (1976) and HARPER (1978). At the 430 MHz Arecibo operating frequency, mesospheric returns must arise from thermal scatter, since the equivalent 37 cm backscattering wavelength is much smaller than the minimum scale of turbulence (see Fig. 8 and RASTOGI and BOWHILL, 1976a). Harper's results, which go down to about 65 km, yield an estimate of the electron density profile as well as series of spectra showing the inferred horizontal velocity of the ion-neutral background. Figure 22 is a profile of the zonal wind between 65–87 km obtained by scaling the mean spectral shift shown in Fig. 1 of HARPER (1978).

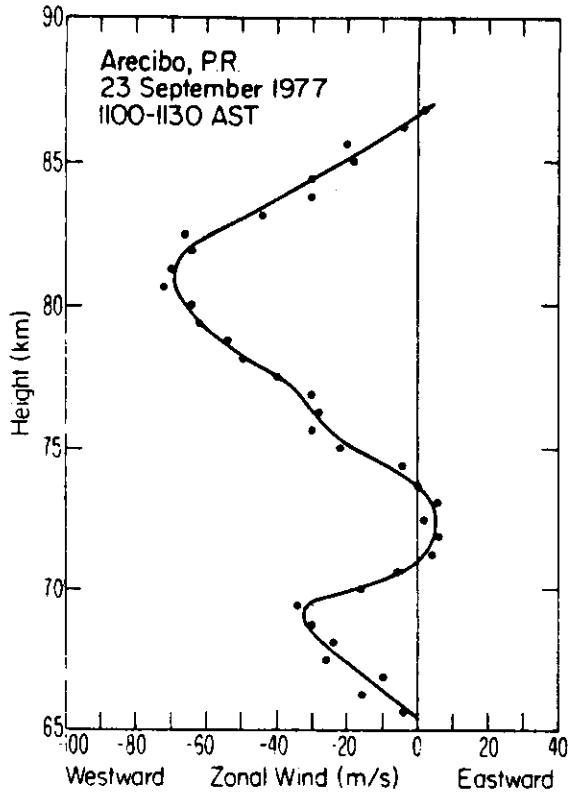

Figure 22
Vertical profile of mesospheric zonal wind observed by the Arecibo radar on 23 September 1977. (Deduced from HARPER, 1978.)

b. Non-thermal scattering

Earliest evidence of enhanced VHF backscattering from mesospheric heights was reported by BOWLES (1961) using a high powered 41 MHz radar in Illinois. He found enhanced echoing strata at a number of heights between 55–85 km, and inferred horizontal velocities of about 20 m/s from the signal fading rate. Similar strata between 70–80 km at equatorial latitudes (Jicamarca) were reported by FLOCK and BALSLEY (1967) who attributed the echoes to turbulent scattering in the presence of an electron density gradient.

The potential of using sensitive VHF radars to study both the total wind field and turbulent processes in the mesosphere was first appreciated by WOODMAN and GUILLÉN (1974) in their pioneering work at Jicamarca. Excellent time resolution records of the wind field showed not only mean and tidal components but also revealed the presence of strong velocity perturbations arising from gravity waves. An example of these perturbations taken from their paper is given in Fig. 23. Woodman and Guillén were able to explain their results in the mesosphere as well as the strato sphere n terms of a scattering mechanism based on neutral atmospheric turbulenc (produced by wind shear) working on the height gradient of the refractive index.

Further studies of the intermittent nature of the mesospheric echoes at Jicamarca and the relationship of the velocity fluctuations to gravity waves were reported by RASTOGI and WOODMAN (1974) for a single mesospheric height. RASTOGI and BOWHILL (1975b) studied the gravity-wave oscillations, showing the dominant wave period to be 10–20 minutes, and inferring the horizontal wavelength to be 200–300 km. In a subsequent study RASTOGI and BOWHILL (1976c) showed that horizontally stratified regions of intermittent turbulence (with vertical dimensions of a few tens of meters) have horizontal dimensions roughly an order of magnitude less than the dominant internal gravity wave scale.

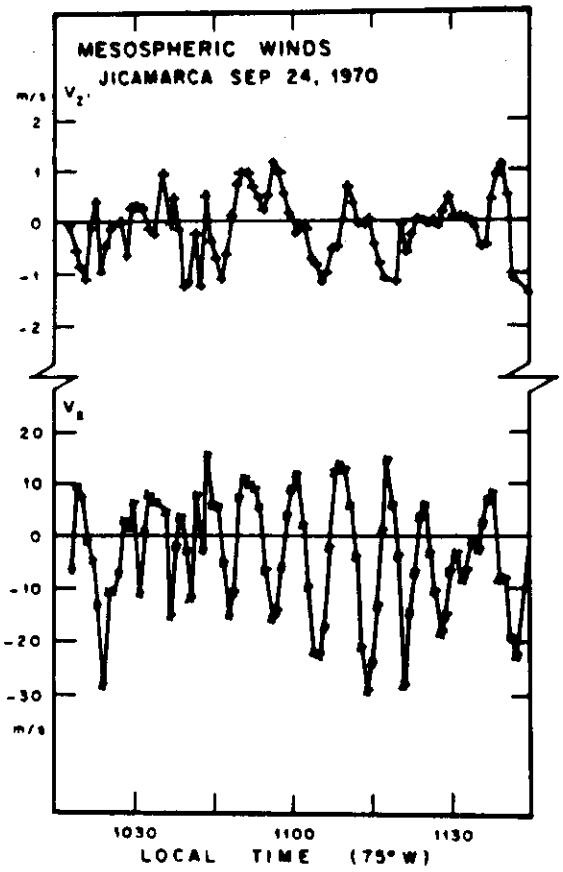

Figure 23
Example of gravity-wave velocity fluctuations obtained by the Jicamarca radar on 24 September 1970. V_x is zonal component and V_z is quasi-vertical. Height resolution is about 5 km. (After WOODMAN and GUILLÉN, 1974.)

Following the installation of a more versatile data processing system at Jicamarca that allowed for simultaneous multiheight analysis, HARPER and WOODMAN (1977) described the stratified nature of the mesospheric echoes and discussed their discontinuous spatial structure. The multiheight capability also produced zonal wind profiles between 65–85 km which supported the earlier conclusion (RASTOGI and WOODMAN, 1974) that the semidiurnal tide over Jicamarca is small.

Increased interest in mesospheric processes during the past few years has led to a series of VHF radar studies at a number of facilities. Essentially continuous measurements of scattered power and radial velocity between 60–90 km for many daytime hours using the Urbana radar have been reported by MILLER *et al.* (1978). An example of strong gravity wave activity is shown in Fig. 24 (Fig. 1 in MILLER *et al.*, 1978). Periods on the order of minutes are apparent in this example.

FUKAO *et al.* (1979) have recently compared mesospheric zonal wind profiles between 62–85 km measured by the Jicamarca radar (12°S latitude) with profiles between 40–65 km measured by meteorological rockets at Ascension Island (8°S latitude) during the same season. This comparison appears in Fig. 25. The good agreement in the region of overlap has been taken by FUKAO *et al.* (1979) as confirmation that the radar indeed measures neutral wind. Figure 19 (also from FUKAO *et al.*, 1979) shows that mesospheric echoes below 70 km (or sometimes somewhat higher) are stronger when observed with a vertically directed antenna – a feature noted previously in troposphere-stratosphere returns by GAGE and GREEN (1978) and RÖTTGER and LIU (1978) and ascribed to Fresnel reflection.

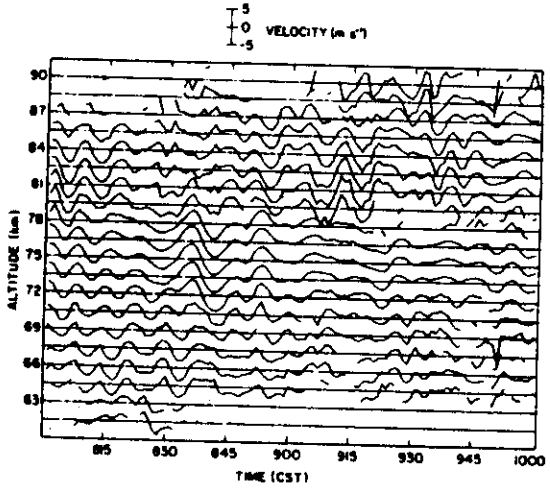

Figure 24
Mesospheric radial velocities observed by the Urbana, Illinois, radar on 11 April 1978. Antenna beam direction is approximately 1.5° from vertical toward the southeast. (After MILLER *et al.*, 1978.)

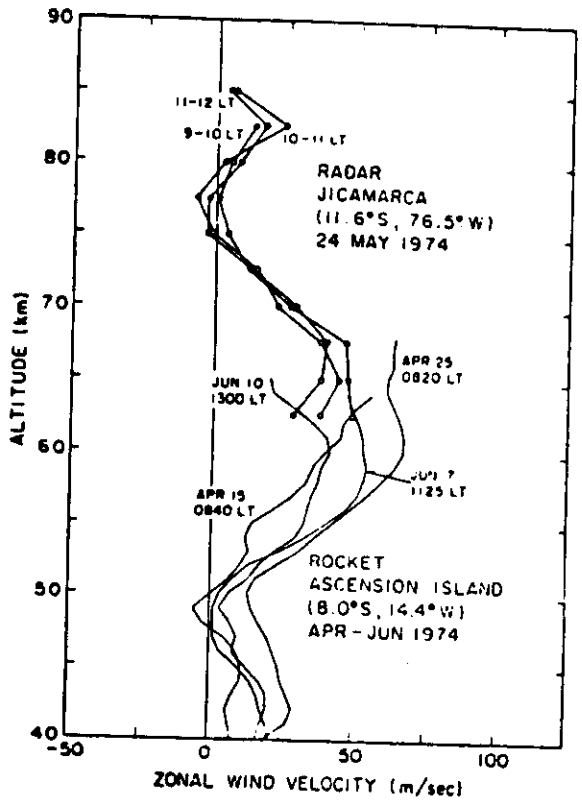

Figure 25
Comparison of zonal wind velocities by the Jicamarca radar (9–12 UT, 24 May 1974) and rockets at Ascension Island (April–June 1974). (After FUKAO *et al.*, 1979.)

High resolution (≃150 m) VHF radar studies of turbulent mesospheric structure using the SOUSY radar have recently been reported by RÖTTGER *et al.* (1979). Their results show three separate types of turbulent structure: blobs and sheets, which are sporadic in nature, only a few hundred meters thick, and which occur preferentially between 60–70 km; and layers, which are thicker (≃2 km) and which occur above 70 km. RÖTTGER *et al.* (1979) also discuss the possibility of Fresnel reflection contributions below 70 km.

Recent mesospheric results from the prototype MST radar at Platteville have been reported by ECKLUND *et al.* (1979). In addition to the strong day-to-day and hour-to-hour variability of the scattered power reported by many investigators, occasional measurements of the zonal wind component were obtained with relatively good time resolution. Figure 26 (from ECKLUND *et al.*, 1979), shows an example of the mesospheric zonal wind. A major feature of the Platteville radar is that it is run on a virtually unattended basis: it was only necessary to visit the site every few days to change data tapes.

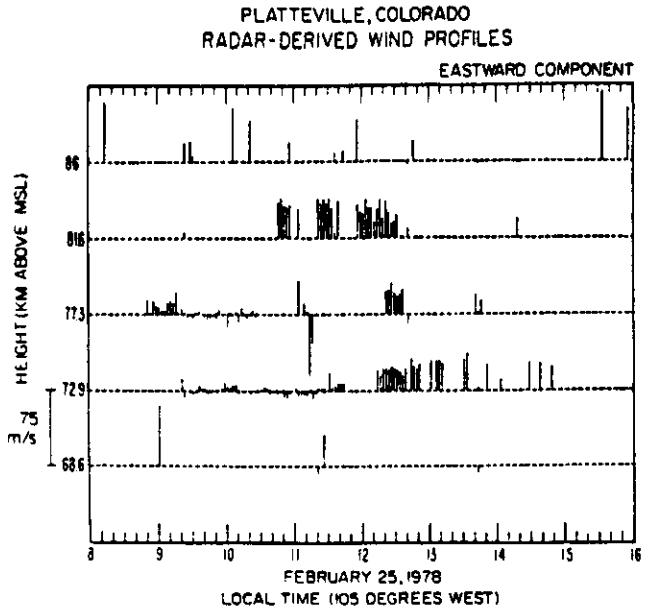

Figure 26
Mesospheric velocities observed by the Platteville radar on 25 February 1978. Scale appears on left. (After ECKLUND *et al.*, 1979.)

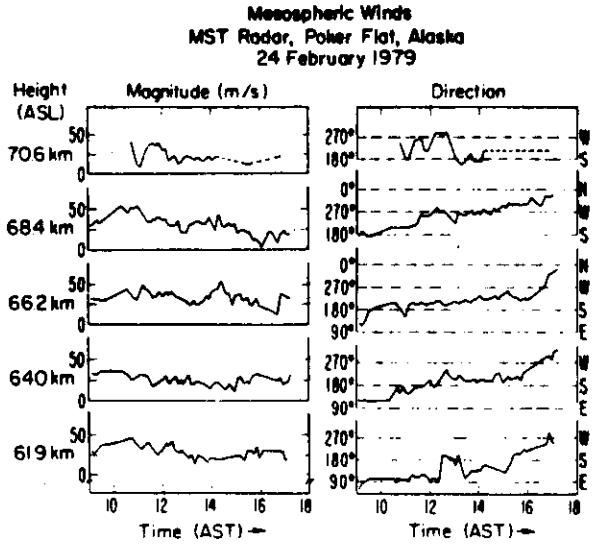

Figure 27
Horizontal mesospheric winds observed by the Poker Flat MST radar on 24 February 1979. Direction refers to the azimuth from which the wind is coming. (After BALSLEY *et al.*, 1979.)

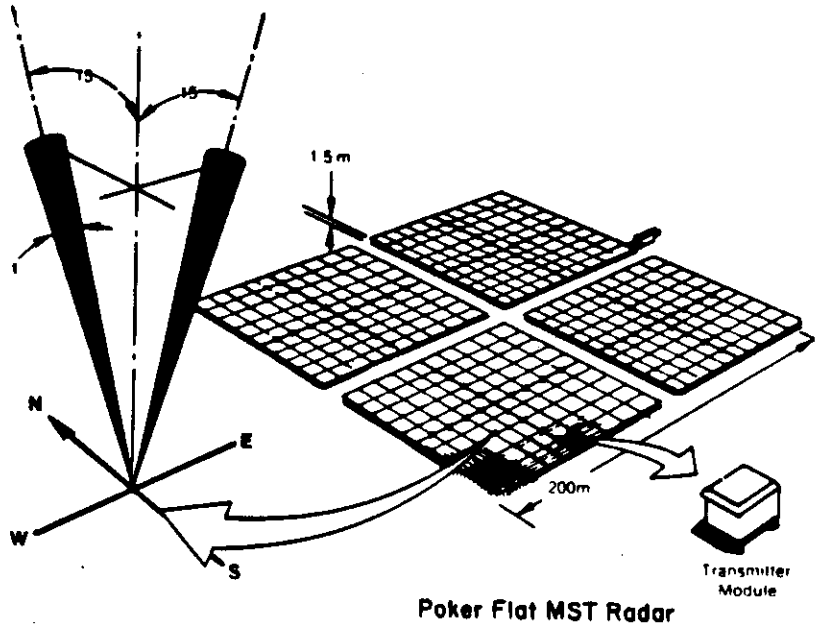

Figure 28
Artist's conception of the complete Poker Flat MST radar.

A seasonal variability in the height of the predominant mesospheric ech region has been reported by CZECHOWSKY *et al.* (1979) using the SOUSY r These authors report that the region of maximum echoes in winter is 70–80 and although echoes from this region are occasionally observable in summer, t :s an additional stronger region of echoes between 80–90 km during summer.

Finally, a continuous eight hour record of high-latitude mesospheric winc the height range 62–71 km obtained by the MST radar under construction at P Flat, Alaska, is shown in Fig. 27 (BALSLEY *et al.*, 1979). The general trend of soutl to westerly flow, from noon to sunset seen in Fig. 27 was observed during a pe of moderate ionospheric absorption (2–3 db at 30 MHz), so that the mesospl ionization density was somewhat enhanced (PARTHARSARTHY *et al.*, 1963). antenna configuration for the Poker Flat MST system, shown in Fig. 28, consis two superimposed but independent dipole arrays that are phased to produce orthogonal beams fifteen degrees from vertical. The system is being designe operate on a nearly continuous, relatively unattended basis. Although these were obtained with the system operating at greatly reduced sensitivity (three or cf magnitude less than the eventual system), they demonstrate the potential of M systems for making continuous observations.

6. *Concluding remarks*

This paper was intended to examine the potential of the MST radar technique for studies of the middle atmosphere. Toward this end we have attempted to review the large body of literature that has already been written.

It appears that there is an unparalleled opportunity to study atmospheric dynamics between the ground and an altitude of about 100 km using the MST technique.

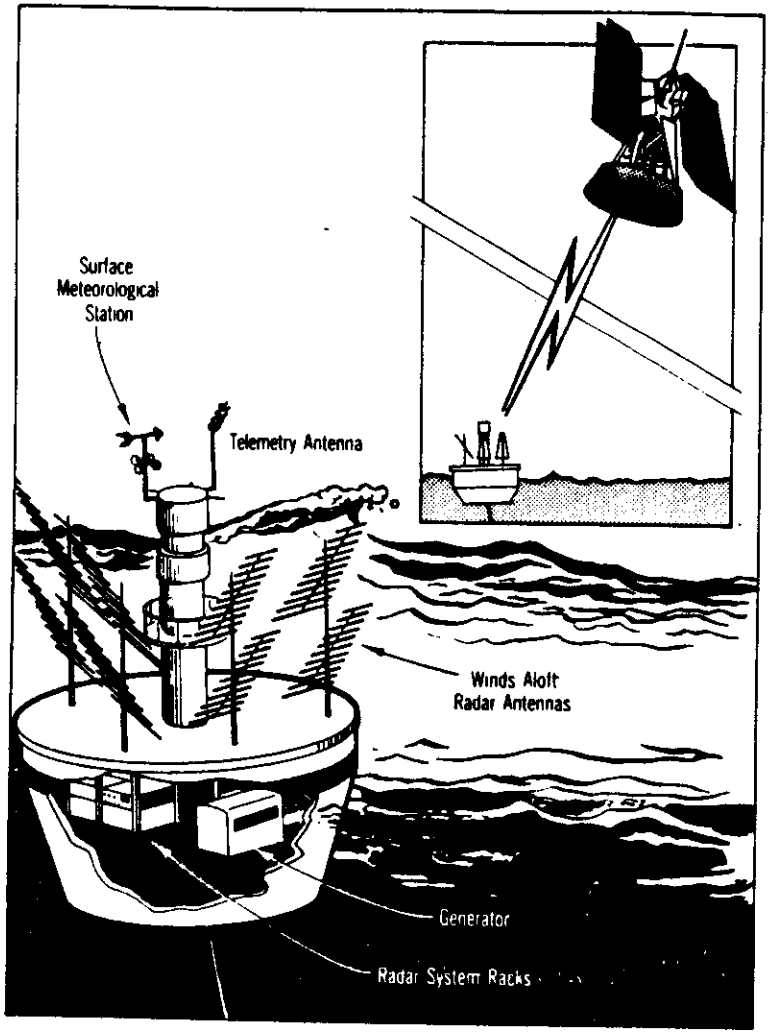

Figure 29
Artist's conception of a small ST radar mounted on an ocean buoy. Currently, radars of this size are capable of continuously measuring winds, waves and turbulence up to at least 15 km with 2 km resolution (cf. Fig. 11).

Topics ranging from the general circulation of the atmosphere to the dynamic coupli between the troposphere, stratosphere and mesosphere, and the morphology atmospheric waves and turbulence are all amenable to study by MST/ST radars.

While the future for MST studies looks bright, there are a number of proble that need to be addressed: (1) except for particle precipitation events and for meteo scatter above about 75 km, mesospheric echoes occur only during the daytime; (although high resolution ($\simeq$ 100 m) sounding is possible in the lower atmosphere a at some mesospheric heights, such resolution over the complete height range wou recuire extremely sensitive radars if the echoing regions are distributed and n stratified; (3) while the cost of an ST radar is moderate (~$100K), the cost of MST facility is in the vicinity of $1000K; (4) MST observations of winds and turb lence parameters have yet to be sufficiently corroborated by other techniques (i balloons, rockets, satellites, partial reflection drift facilities, etc.). This problem specially acute in the mesosphere.

As of this writing, troposphere-stratosphere research using MST and ST rada is more active than mesospheric research. This is due in part to the proliferation of t less expensive ST radars. Research activities in the higher heights should increase wit the completion of a number of proposed MST systems (i.e., Poker Flat, MU, an Urbana).

Should the problems listed above be satisfactorily resolved, then a nested networ of operational MST/ST radar systems (similar to the current configuration of th NWS radiosonde and MRN rocket sites) becomes attractive. In this configuration the MST radars would provide information on winds, waves and turbulence betwee 1–100 km on a coarse grid and the ST radars would serve as intermediate monitor of the troposphere and lower stratosphere on a smaller spatial grid. Clearly this i an ambitious concept and one that will require a large investment in time and mone to achieve. On the other hand, estimates of the costs of individual MST or ST systems when amortized over many years, are not excessive, particularly when one consider the relatively unattended operation and the continuous data taking capability.

A future MST/ST network could nicely complement the existing meteorologica monitoring network by providing continuous measurements of winds, waves and turbulence. In this connection it should be recognized that the radar technique by itself is incapable of providing temperature, and humidity by conventional sounding techniques.[3])

It is reasonable to expect that future ST radar systems will be more-or-less portable and will be capable of observing to greater heights. Calculations based on existing data show that portable systems capable of producing averaged profiles similar to those shown in Fig. 11 up to at least 15 km can be designed in the lower UHF range

[3]) A hybrid ground-based system (consisting of an ST radar to measure wind profiles and a microwave radiometer (DECKER *et al.*, 1978) to measure temperature and humidity profiles) could operate to measure winds, temperature, and humidity on a relatively continuous basis (LITTLE, private communication).

using an array of four yagi-uda antennas and a total physical area of less than 150 m². An example of such a system is shown in Fig. 29. While this figure shows a system installed on an ocean buoy, similar systems could operate equally well on land. A number of such systems might operate temporarily, for example, in a tight grid to obtain data for mesoscale studies (e.g., orographic effects, sea-land interface, severe storms).

Operation at frequencies < 40 MHz has yet to be fully examined. While there are a number of inherent problems (ionospheric reflections, radio-frequency spectrum contamination, less spatial resolution and higher background noise) in operating at lower frequencies, the early experiments of Watson-Watt and extrapolations from current VHF studies indicate that scattering and Fresnel reflections may be considerably stronger at lower frequencies.

The capability of measuring vertical velocities on a continuous basis should also be emphasized. For example, proposed solutions for a number of unanswered mesospheric problems (e.g., the generation of noctilucent clouds, and the occurrence of a cold summertime mesosphere) require relatively large vertical velocities. Similarly, measurements of vertical velocities in the troposphere-lower stratosphere can yield important information on a variety of dynamical phenomena.

Finally, it is worthwhile mentioning the idea of examining possible Sun-weather relationships. It is reasonable to expect that a correlation between solar variability and weather – if indeed a correlation exists – will be manifested in middle atmosphere patterns of winds and waves. Continuous observations of these parameters by MST radars, particularly in the auroral zone where ionospheric effects of solar variability are most pronounced, will provide an ideal data base for such studies.

7. *Acknowledgements*

We are happy to acknowledge many useful and interesting discussions with T. E. VanZandt, J. L. Green, W. L. Ecklund and D. A. Carter of the Aeronomy Laboratory, NOAA, and with R. F. Woodman (Arecibo Observatory) and R. M. Harper (Rice University). We are also indebted to Mrs. H. Axtell for her prompt and efficient typing of the manuscript. This research was partially supported by the Atmospheric Research Section of the National Science Foundation.

References

Balsley, B. B. and Ecklund, W. L. (1972), *A portable coaxial collinear antenna*, IEEE Transactions on Antennas and Propagation, AP-20, 513–516.

Balsley, B. B., Cianos, N., Farley, D. T. and Baron, M. J. (1977), *Winds derived from radar measurements in the Arctic troposphere and stratosphere*, J. Appl. Meteor. *16*, 1235–1239.

Balsley, B. B. (1978), *The use of sensitive coherent radars to examine atmospheric parameters in the height range 1–100 km*, Preprints, 18th Conf. on Radar Meteorology (Atlanta) AMS, Boston, pp. 190–193.

Balsley, B. B., Ecklund, W. L., Carter, D. A. and Johnston, P. E. (1979), *The Poker Flat MST radar: First results*, Geophys. Res. Letters, in press.

Bean, B. R. and Dutton, E. J. (1968), *Radio Meteorology* (Dover, New York) 435 pp.

Belrose, J. S. (1970), *Radio wave probing of the ionosphere by the partial reflection of radio wav (from heights below 100 km)*, J. Atmos. Terr. Phys. *32*, 567–596.

Booker, H. G. and Gordon, W. E. (1950), *Theory of radio scattering in the troposphere*, Pro IEEE *38*, 401–412.

Bowles, K. L. (1961), *Incoherent scattering by free electrons as a technique for studying the ion sphere and exosphere: Some observations and theoretical considerations*, J. Res. Natl. Bu Standards *65D*, 1–14.

Chisholm, J. H., Portmann, P. A., Debettencourt, J. T. and Roche, J. F. (1955), *Investigation of angular scattering and multipath properties of tropospheric propagation of short radio wave beyond the horizon*, Proc. IEEE *43*, 1317–1335.

Colwell, R. C. and Friend, A. W. (1936), *The D-region of the ionosphere*, Nature *137*, 782.

Cunnold, D. M. (1975), *Vertical transport coefficients in the mesosphere obtained from rada observations*, J. Atmos. Sci. *32*, 2191–2200.

Czechowsky, P., Rüster, R. and Schmidt, G. (1979), *Variations of mesospheric structures o different seasons*, Geophys. Res. Lett. *6*, 459–462.

Decker, M. T., Westwater, E. R. and Guiraud, F. O. (1978), *Experimental evaluation of ground based microwave radiometric sensing of atmospheric temperature and water vapor profiles*, J App . Meteor. *17*, 1788–1795.

Donn, W. L. and Rind, D. (1972), *Microbaroms and the temperature and wind of the upper atmosphere*, J. Atmos. Sci. *29*, 156–172.

Ecklund, W. L., Carter, D. A. and Gage, K. S. (1977), *Sounding of the lower atmosphere with a portable 50 MHz coherent radar*, J. Geophys. Res. *82*, 4969–4971.

Ecklund, W. L., Carter, D. A. and Balsley, B. B. (1979), *Continuous measurement of upper atmospheric winds and turbulence using a VHF Doppler radar: Preliminary results*, J. Atmos. Terr. Phys., in press.

Ellsaesser, H. W. (1969), *A climatology of epsilon (atmospheric dissipation)*, Mon. Wea. Rev. *97*, 415–423.

Evans, J. V. (1969), *Theory and practice of ionosphere study by Thomson scatter radar*, Proc. IEEE *57*, 496–500.

Evans, J. V. (1974), *Some post-war developments in ground-based radiowave sounding of the ionosphere*, J. Atmos. Terr. Phys. *36*, 2183–2234.

Farley, D. T., Balsley, B. B., Swartz, W. E. and La Hoz, C. (1979), *Winds aloft in the tropics measured by the Arecibo radar*, J. Appl. Meteor. *18*, 227–230.

Flock, W. L. and Balsley, B. B. (1967), *VHF radar returns from the D region of the equatorial ionosphere*, J. Geophys. Res. *72*, 5537–5541.

Friend, A. W. (1949), *Theory and practice of tropospheric sounding by radar*, Proc. IEEE *37*, 116–138.

Frisch, A. S. and Clifford, S. F. (1974), *A study of convection capped by a stable layer using Doppler radar and acoustic echoes sounders*, J. Atmos. Sci. *31*, 1622–1627.

Frisch, A. S. and Strauch, R. G. (1976), *Doppler radar measurements of turbulent kinetic energy dissipation rates in a Northeastern Colorado convective storm*, J. Appl. Meteor. *15*, 1012–1017.

Fukao, S., Kato, S., Yokoi, S., Harper, R. M., Woodman, R. F. and Gordon, W. E. (1978), *One full-day radar measurement of lower stratosphere winds over Jicamarca*, J. Atmos. and Terr. Phys. *40*, 1331–1337.

Fukao, S., Sato, T., Kato, S., Harper, R. M., Woodman, R. F. and Gordon, W. E. (1979), *Mesospheric winds and waves over Jicamarca on 23–24 May 1974*, submitted to J. Geophys. Res.

Gage, K. S., Birkemeifr, W. P. and Jasperson, W. H. (1973), *Atmospheric stability measurements at tropopause altitudes using forward-scatter CW radar*, J. Appl. Meteor. *12*, 1205–1212.

Gage, K. S. and Balsley, B. B. (1978), *Doppler radar probing of the clear atmosphere*, Bull. Am. Meteor. Soc. *59*, 1074–1093.

Gage, K. S. and Clark, W. L. (1978), *Mesoscale variability of jet stream winds observed by the Sunset VHF Doppler radar*, J. Appl. Meteor. *17*, 1412–1416.

GAGE, K. S. and GREEN, J. L. (1978), *Evidence for specular reflection from monostatic VHF radar observations of the stratosphere*, Radio Sci. *13*, 991–1001.

GAGE, K. S., GREEN, J. L. and VANZANDT, T. E. (1978), *Vertical profiles of C_n^2 in the free atmosphere*, Preprints, 18th Conf. on Radar Meteorology (Atlanta) AMS, Boston, pp. 80–87.

GAGE, K. S. and GREEN, J. L. (1979), *Tropopause detection by partial specular reflection using VHF radar*, Science *203*, 1238–1240.

GAGE, K. S. (1979), *Evidence for a $k^{-5/3}$ law inertial range in mesoscale two-dimensional turbulence* J. Atmos. Sci. (in press).

GAGE, K. S., GREEN, J. L., CLARK, W. L. and VANZANDT, T. E. (1979), *Doppler radar measurement of turbulence in the clear atmosphere*, Proc. Conf. Fourth Symp. on Turbulence, Diffusion, and Air Pollution (Reno) AMS, Boston, pp. 522–529.

GJESSING, D. T. (1964), *Determination of isotropy properties of the tropospheric permittivity and wind velocity fields by radio-propagation methods*, J. Geophys. Res. *69*, 569–581.

GORDON, W. E. (1978), *Atmospheric dynamics in the 1980's*, Position paper for the 1978 Summer Study Programs of the National Academy of Science Committee on Solar-Terrestrial Research, Rice University, Houston.

GORELICK, A. G. and MEL'NICHUK, YU. V. (1968), *A new method for measuring dissipation rate of turbulence in clouds and precipitation using conventional radar*, Proc. Third All Union U.S.S.R. Radar Meteorology Conf., Israel Program for Scientific Translation, Jerusalem, pp. 150–156.

GRANT, J. R. (1979), *Generation and characteristics of jet-stream associated gravity waves*, Ph.D. Thesis, Univ. of Colo., Boulder.

GREEN, J. L., GAGE, K. S. and VANZANDT, T. E. (1978), *Three-dimensional wind observations of a jet stream using a VHF Doppler radar*, Preprints, 18th Conf. on Radar Meteorology (Atlanta), AMS, Boston, pp. 184–189.

GREEN, J. L., GAGE, K. S. and VANZANDT, T. E. (1979), *Atmospheric measurements by VHF pulsed Doppler radar*, to be published in the Nov. issue of IEEE Transactions on Geoscience Electronics.

GROSSI, M. D., SOUTHWORTH, R. B. and ROSENTHAL, S. K. (1972), *Radar observations of meteor winds above Illinois*, in Thermospheric Circulation (Willis L. Webb, ed., Mass. Institute of Technology), pp. 205–248.

HARDY, K. R., ATLAS, D. and GLOVER, K. M. (1966), *Multiwavelength backscatter from the clear atmosphere*, J. Geophys. Res. *71*, 1537–1552.

HARPER, R. M. and WOODMAN, R. F. (1977), *Preliminary multiheight radar observations of waves and winds in the mesosphere over Jicamarca*, J. Atmos. Terr. Phys. *39*, 959–963.

HARPER, R. M. (1978), *Preliminary measurements of the ion component of the incoherent scatter spectrum in the 70–90 km region over Arecibo*, Geophys. Res. Lett. *5*, 784–786.

HUNSUCKER, R. D. (1974), *Simultaneous Riometer and incoherent scatter radar observations of the auroral D region*, Radio Sci. *9*, 335–340.

KRAICHNAN, R. H. (1967), *Inertial ranges in two-dimensional turbulence*, Phys. Fluids *10*, 1417–1423.

KROPFLI, R. A., KATZ, I., KONRAD, T. G. and DOBSON, E. B. (1968), *Simultaneous radar reflectivity measurements and refractive index spectra in the clear atmosphere*, Radio Sci. *3*, 991–994.

KROPFLI, R. A. (1971), *Simultaneous radar and instrumented aircraft observations in a clear air turbulent layer*, J. Appl. Meteor. *10*, 796–802.

LANE, J. A. and SOLLUM, P. W. (1965), *VHF transmission over distances of 140 and 300 km*, Proc. IEEE, London, *112*, 254–258.

LANE, J. A. (1969), *Radar echoes from clear air in relation to refractive-index variations in the troposphere*, Proc. IEEE, London *116*, 1656–1660.

LILLY, D. K., WACO, D. E. and ADELFANG, S. I. (1974), *Stratospheric mixing estimated from high-altitude turbulence measurements*, J. Appl. Meteor. *13*, 488–493.

MATHEWS, J. D. (1976), *Measurements of diurnal tides in the 80- to 100-km altitude range at Arecibo*, J. Geophys. Res. *81*, 4671–4677.

MEGAW, E. C. S. (1957), *Fundamental radio scatter propagation theory*, Institute of Elec. Eng. Proc., *104*, Part C6, 441–456 (Monograph No. 236R).

METCALF, J. I. and ATLAS, D. (1973), *Microscale ordered motions and atmospheric structure associated with thin echo layers in stably stratified zones*, Boundary Layer Meteor. *4*, 7–35.

MILLER, K. L., BOWHILL, S. A., GIBBS, K. P. and COUNTRYMAN, I. D. (1978), *First measurements of mesospheric vertical velocities by VHF radar at temperate latitudes*, Geophys. Res. Lett. *5*, 939–942.

PARTHASARATHY, R., LERFALD, G. M. and LITTLE, C. G. (1963), *Derivation of electron-density profiles in the lower ionosphere using radio absorption measurements at multiple frequencies*, J. Geophys. Res. *68*, 3581–3588.

PETERSON, V. L. and BALSLEY, B. B. (1980), *Clear air Doppler radar measurements of the vertical component of wind velocity in the troposphere and stratosphere*, Geophys. Res. Lett., in press.

PROBERT-JONES, J. R. (1962), *The radar equation in meteorology*, Quart. J. Roy. Met. Soc. *88*, 485–495.

RASTOGI, P. K. and WOODMAN, R. F. (1974), *Mesospheric studies using the Jicamarca incoherent-scatter radar*, J. Atmos. Terr. Phys. *36*, 1217–1231.

RASTOGI P. K. and BOWHILL, S. A. (1976a), *Scattering of radio waves from the mesosphere – 1. Theory and observations*, J. Atmos. Terr. Phys. *38*, 399–411.

RASTOGI. P. K. and BOWHILL, S. A. (1976b), *Gravity waves in the equatorial mesosphere*, J. Atmos. Terr. Phys. *38*, 51–60.

RASTOGI. P. K. and BOWHILL, S. A. (1976c), *Scattering of radio waves from the mesosphere – 2. Evidence for intermittent mesospheric turbulence*, J. Atmos. Terr. Phys. *38*, 449–462.

REAGAN, J. B. and WATT, T. M. (1976), *Simultaneous satellite and radar studies of the D region ionosphere during the intense solar particle events of August 1972*, J. Geophys. Res. *81*, 4579–4596.

ROPER, R. G. (1977), *Turbulence in the lower thermosphere*, in *The Upper Atmosphere and Magnetosphere*, National Academy of Sciences, Washington, D.C.

RÖTTGER J. and LIU, C. H. (1978), *Partial reflection and scattering of VHF radar signals from the clear atmosphere*, Geophys. Res. Lett. *5*, 357–360.

RÖTTGER J. and VINCENT, R. A. (1978), *VHF radar studies of tropospheric velocities and irregularities using spaced antenna techniques*, Geophys. Res. Lett. *5*, 917–920.

RÖTTGER, J., RASTOGI, P. K. and WOODMAN, R. F. (1979), *High-resolution VHF radar observations of turbulence structures in the mesosphere*, Geophys. Res. Lett. *6*, 617–620.

RÜSTER, R., RÖTTGER, J. and WOODMAN, R. F. (1978), *Radar measurements of waves in the lower stratosphere*, Geophys. Res. Lett. *5*, 555–558.

SAXTON, J. A., LANE, J. A., MEADOWS, R. W. and MATTHEWS, P. A. (1964), *Layer structure of the troposphere – Simultaneous radar and microwave refractometer investigations*, Proc. IEE *111*, 275–283.

TATARSKI, V. I. (1971), *The effects of the turbulent atmosphere on wave propagation*, U.S. Dept. of Commerce, pp 74–76.

VANZANDT, T. E., GREEN, J. L., GAGE, K. S. and CLARK, W. L. (1978), *Vertical profiles of refractivity turbulence structure constant: Comparison of observations by the sunset radar with a new theoretical model*, Radio Sci. *13*, 819–829.

VANZANDT, T. E., GREEN, J. L. and CLARK, W. L. (1979), *Buoyancy waves in the troposphere: Doppler radar observations and a theoretical model*, Geophys. Res. Lett. *6*, 429–432.

WAIT, J. R. (1962), *Electromagnetic Waves in Stratified Media* (Pergamon Press, London) Chapter IV.

WATSON-WATT, R. A., WILKINS, A. F. and BOWEN, E. G. (1937), *The return of radio waves from the middle atmosphere – 1*, Proc. Roy. Soc. A *161*, 181–196.

WHEELON, A. D. (1960), *Relation of turbulence theory to ionospheric forward scatter propagation experiments*, J. Res. NBS *64D* (Radio Prop.), 301–309.

WOODMAN, R. F. and GUILLÉN, A. (1974), *Radar observations of winds and turbulence in the stratosphere and mesosphere*, J. Atmos. Sci. *31*, 493–505.

YEH, K. C. and LIU, C. H. (1972), *Theory of Ionospheric Waves*, Academic Press, New York, 464 pages.

(Received 15th June 1979)